
NeuralThink: Algorithm Synthesis that Extrapolates in General Tasks

Bernardo Esteves^{1,2} Miguel Vasco³ Francisco S. Melo^{1,2}

Abstract

While machine learning methods excel at pattern recognition, they struggle with complex reasoning tasks in a scalable, algorithmic manner. Recent Deep Thinking methods show promise in learning algorithms that *extrapolate*: learning in smaller environments and executing the learned algorithm in larger environments. However, these works are limited to symmetrical tasks, where the input and output dimensionalities are the same. To address this gap, we propose NeuralThink, a new recurrent architecture that can consistently extrapolate to both symmetrical and asymmetrical tasks, where the dimensionality of the input and output are different. We contribute with a novel benchmark of asymmetrical tasks for extrapolation. We show that NeuralThink consistently outperforms the prior state-of-the-art Deep Thinking architectures, in regards to stable extrapolation to large observations from smaller training sizes.

1. Introduction

Humans can solve complex reasoning tasks by *extrapolating*: employing and combining elementary logical components to build more elaborate strategies. Modern machine learning models excel at pattern recognition, often outperforming humans in classification (He et al., 2015; 2016), control (Mnih et al., 2013) and prediction tasks (Jumper et al., 2021). However, these models still struggle at reasoning tasks, hindering their ability to maintain their performance for increasingly higher difficulty versions of the same task (Schwarzschild et al., 2021). A particular type of difficulty emerges from the increase in *dimensionality* of the input. As shown in Figure 1, learning to perform decision-making tasks becomes increasingly harder as the observation space of the agent increases.

We focus on designing learning algorithms that are able

¹INESC-ID, Lisbon, Portugal ²Instituto Superior Técnico, University of Lisbon, Portugal ³KTH Royal Institute of Technology, Stockholm, Sweden. Correspondence to: Bernardo Esteves <bernardo.esteves@tecnico.ulisboa.pt>.

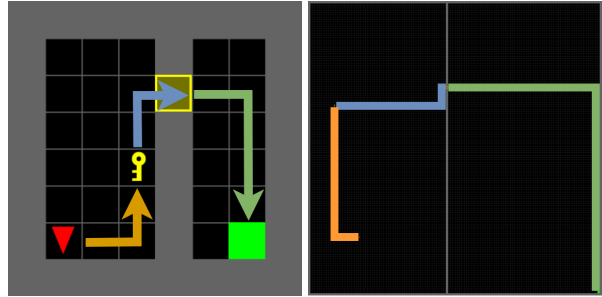


Figure 1: Observations of the `Doorkey` environment of sizes 8×8 and 128×128 , where the agent must pick up the key (orange), open the door (blue) and go to the goal (green). In this work, we propose **NeuralThink**, a novel Deep Thinking architecture that is able to train on the small environment (left) and extrapolate to the large environment (right) without loss in performance or fine-tuning.

to efficiently extrapolate over inputs, i.e., are able to train over small dimensional observations and execute over arbitrarily high dimensional observations, without a significant loss in performance nor additional fine-tuning. Recently, several Deep Thinking methods have been proposed that employ recurrent neural networks to mimic the extrapolation process (Schwarzschild et al., 2021; Bansal et al., 2022). Compared to feed-forward networks, which have finite depth, recurrent networks can be iterated to an arbitrary depth after the training procedure. This architectural choice allows algorithms to extrapolate to significantly larger input dimensions without suffering from collapse due to excessive iterations, a problem known as *overthinking* (Bansal et al., 2022). However, to the best of our knowledge, all prior Deep Thinking methods that are able to extrapolate to large input sizes have assumed that the output size of the network is equal to its input size. As such, the application of these methods is currently restricted to *symmetrical* tasks, such as image generation.

We address this limitation and propose a novel architecture able to consistently extrapolate regardless of the size of the output. We contribute *NeuralThink*, an efficient architecture which can be employed in both symmetrical and *asymmetrical* tasks (e.g., classification, reinforcement learning tasks), when provided with images of arbitrary size at execution time, despite never having trained over such

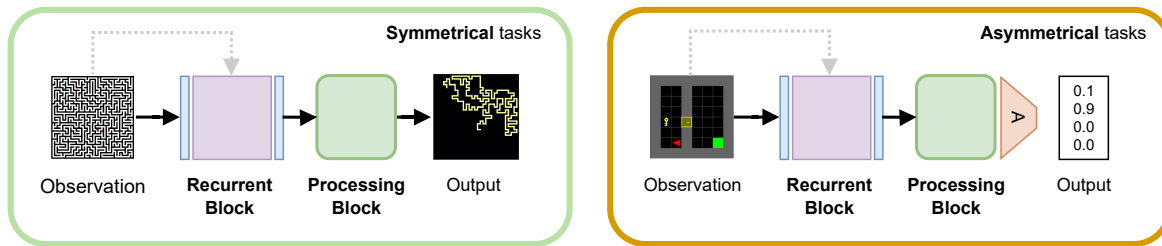


Figure 2: NeuralThink is a Deep Thinking architecture composed of two main components. The recurrent convolutional block (depicted in purple) is responsible for propagating information across the observation (or arbitrary size) by performing multiple iterations of its latent space. At each iteration we provide the original observation to the recurrent block. The processing block (depicted in green), with an optional aggregation layer (A), is responsible for generating the output. Contrary to prior Deep Thinking architectures, NeuralThink can be employed in both symmetrical (left) and asymmetrical (right) tasks to provide consistent extrapolation.

images. Our simple approach combines a recurrent convolutional block, able to perceive information at different scales in the provided image through multiple iterations, and a processing block (with an aggregation function), responsible for merging the perceived information in the model. We train NeuralThink on a collection of lower-dimensional observations using standard supervised learning techniques, and apply the learned algorithm at test time with arbitrarily large observations.

We evaluate NeuralThink against prior Deep Thinking architectures in symmetrical tasks and show that NeuralThink outperforms previous approaches both in terms of extrapolation capabilities (being able to execute over larger image input sizes) but also in terms of training efficiency (being able to train over smaller image input sizes). Additionally, we contribute with a novel benchmark of asymmetrical tasks to evaluate the extrapolation capabilities of Deep Thinking models in environments with different input and output sizes. Once again, the results show that NeuralThink significantly outperforms the baselines in extrapolation capabilities and training efficiency.

In summary, the contributions of our work are:

- **NeuralThink:** We propose a novel Deep Thinking architecture that uses a recurrent convolutional block and an processing block (with an aggregation function) to allow consistent extrapolation in symmetrical and asymmetrical tasks to arbitrary input sizes;
- **Asymmetrical Benchmark:** We contribute with a novel benchmark of asymmetrical classification tasks for Deep Thinking architectures, which provide image observations of arbitrary size;
- **Consistent Extrapolation:** We show that NeuralThink outperforms the prior Deep Thinking architectures regarding stable extrapolation to large observations and training efficiency.

2. Related Work

Algorithmic Learning The use of recurrent neural networks to learn algorithms has been explored in prior work, with the introduction of Neural Turing Machines (Graves et al., 2014; Zaremba & Sutskever, 2015), Neural GPUs (Kaiser & Sutskever, 2016; Price et al., 2016; Freivalds & Liepins, 2017), Neural Arithmetic Logic Units (Trask et al., 2018), and Deep Thinking networks (Schwarzschild et al., 2021; Bansal et al., 2022). Some of these models show promising results in array-based (Schwarzschild et al., 2021; Bansal et al., 2022) and graph-based algorithm learning (Velickovic et al., 2022; Bevilacqua et al., 2023; Ibarz et al., 2022). In this work, we focus in algorithm learning for array-based structures.

Deep Thinking Networks (Schwarzschild et al., 2021) introduced the concept of Deep Thinking networks, a class of recurrent neural networks that can execute at test time more iterations than the number of iterations used during training, to solve problems more complex than the ones seen during training. The authors also introduced a benchmark of algorithm learning tasks, where the input and output are represented as arrays of the same size. We refer to these tasks as *symmetrical* tasks, since the input and output have the same dimensionality. As a model, they propose a recurrent network architecture based on ResNets (He et al., 2016) that demonstrates logical extrapolation abilities across the proposed symmetrical benchmarks while leveraging the spatial invariances in the inputs. However, these networks suffer from a problem called *overthinking*, where the network deteriorates in performance when the number of iterations is extended beyond the training distribution (Bansal et al., 2022).

(Bansal et al., 2022) proposes the introduction of two components to solve the overthinking problem: (1) a recall module, that integrates the input directly into specific layers of the recurrent network and safeguards against potential

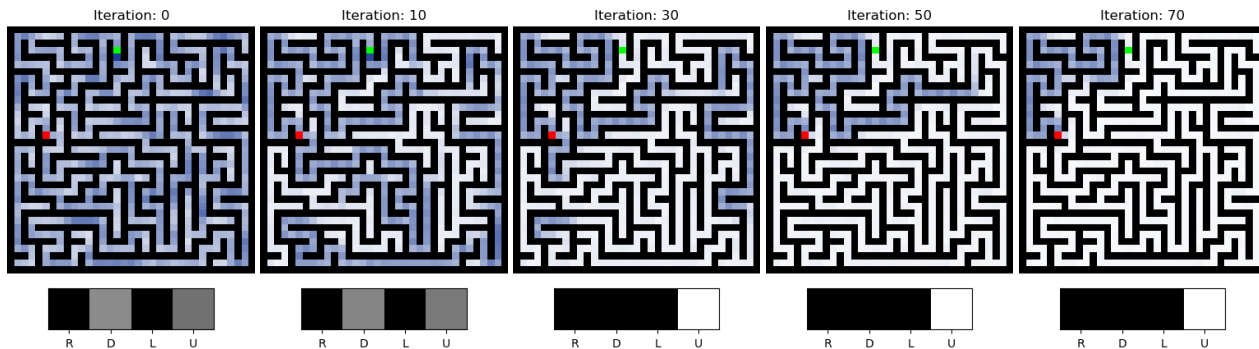


Figure 3: Propagation of information in NeuralThink. Top: difference between the current iteration and last iteration (not represented) of the recurrent state of NeuralThink in a maze-like environment, where the goal is for the agent (red) to find the goal position (green). Higher differences are represented in deep blue color. Bottom: predicted action probabilities outputted by the model at different iterations, where the agent can move right (R), down (D), left (L), or up (U).

loss or corruption of deep features; (2) a progressive loss (PL) training scheme that incentivizes recurrent networks to iteratively refine the feature representation, preventing the network from memorizing the number of recurrent module applications. With these additions, the improved Deep Thinking network is able to extrapolate to problems 16 times larger than the training size with more than 95% accuracy on the symmetrical benchmark. We call this improved architecture *DeepThink* and use it as a baseline against our method. However, *DeepThink* can only be applied to symmetrical tasks.

The use of a progressive loss brings two disadvantages: (1) the loss requires two separate forward passes through the network, increasing the computational cost of the training; (2) the loss parameter needs to be tuned for each problem, which can be a time-consuming process. To address these issues, (Salle & Malmasi, 2023) propose replacing the progressive loss with a delta loss term (Salle & Prates, 2019) and achieve similar performance to *DeepThink*. In this work, we propose a novel Deep Thinking architecture that is able to outperform *DeepThink* without the need of any additional loss to counter the overthinking problem (as shown in Section 5.1).

For an extensive version of the related work, please refer to Appendix E. To the best of our knowledge, we propose the first method to consistently extrapolate learned algorithms to a more general class of tasks.

3. Algorithm Synthesis for Consistent Extrapolation

In this work, we address the problem of learning algorithms that are able to consistently extrapolate to input observations of higher dimensionality. We define two types of extrapolation tasks: *symmetrical* tasks, where the input and output have the same dimensionality, and *asymmetrical* tasks,

where the input and output have different dimensionality. We propose **NeuralThink**, a novel architecture for Deep Thinking methods that is able to consistently extrapolate to higher observations in both symmetrical and asymmetrical tasks. In Figure 2 we present the overall architecture of our method.

3.1. NeuralThink

As shown in Figure 2, NeuralThink is composed of two different modules: a recurrent convolutional module, responsible for iteratively processing the observation, and a processing module, responsible for aggregating (if necessary) and generating the output.

Recurrent Convolutional Module: This module consists of a layernormalized Convolutional LSTM (Shi et al., 2015; Ba et al., 2016), a LSTM that uses convolutional layers instead of linear layers in its recurrent structure. The layer normalization is used to normalize the output of the convolutional layers and the cell state. We always provide the original input observations in the recurrent iterations of the LSTM, thus preventing the network from forgetting the input information over time, similar to the recall module in (Bansal et al., 2022). We maintain the dimensionality of the input and output of this module constant in order to perform multiple iterations over the data, allowing for consistent extrapolation, as shown in Section 5.1.

Processing Module: This module consists of a block of three convolutional layers whose input is the last hidden state of the recurrent block. Their purpose is to reduce the number of channels to a desired output number of channels. Additionally, we have an optional aggregation layer (in our case a global max-pooling layer) that can be employed in asymmetrical tasks to reduce the variable input size of the network to a fixed output size. For example, for a two-dimensional input observation, we first reduce the input to

a $1 \times 1 \times N$ tensor, where N is the desired output number of channels, and subsequently flatten the output tensor.

Training Scheme We train NeuralThink on a set of smaller-dimensional observations and test the performance of the model with larger dimensional observations (all belonging to the same task). Additionally, for asymmetrical tasks we employ a curriculum learning approach, inspired by (Kaiser & Sutskever, 2016; Zaremba & Sutskever, 2014), to counter the effect of the reduced training signal (due to the smaller output dimensionality): we initially train the models on lower-dimensionality observations, and then gradually increase the dimensionality of the observations every N epochs. To reduce the risk of catastrophic forgetting, we sample a minibatch of observations with a previously seen dimensionality (chosen uniformly at random) with a 20% chance. We empirically found this value to be sufficient for the learning procedure.

In Section 5.3, we empirically show the importance of each of these components for the overall performance of NeuralThink. For additional details on the complete architecture, please refer to Appendix B. Additionally, for more details on the used training hyperparameters please refer to Appendix C.¹

3.2. Propagation of Information

To understand the extrapolation process in NeuralThink, and how information propagates along the model, we focus on the value of the internal recurrent state (in the recurrent convolutional module) as a function of the number of iterations. In Figure 3, we present a maze-like environment at different iteration steps and color in dark blue the difference between the current and last iteration of the recurrent state of NeuralThink (more intense for larger differences).

As the number of iterations increases, a larger number of sections in the maze become white, meaning that the hidden state has converged to the same value as the last state. In this sense, what we see in the figure is how the information propagates through the hidden state as we increase the number of iterations. The speed of this propagation depends on the receptive field of the convolution: for example, a single convolution with a kernel size of 3 can capture the information from the adjacent pixels, propagating the information forward in one direction for a single pixel. As such, by using recurrent neural networks we can propagate information, regardless of observation size, by performing an appropriate number of iterations.

This propagation of information also influences the output prediction. In Figure 3 (bottom), we observe that the prediction of the output label is uncertain before iteration #30.

¹The open-source implementation of NeuralThink is available at <https://github.com/esteveste/NeuralThink>

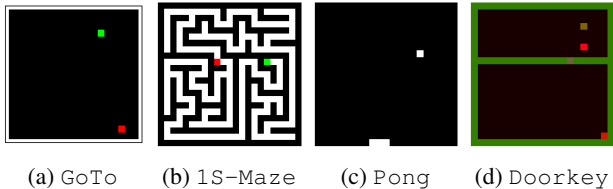


Figure 4: The proposed benchmark of asymmetrical tasks to evaluate the extrapolation performance. In all tasks, the input is an image observation of the environment with arbitrary size. The output is an n -dimensional one-hot vector, corresponding to the next-step actions available to the agent, with: a) $n = 4$; b) $n = 4$; c) $n = 3$; d) $n = 4$.

However, in this iteration, the hidden state near the agent (in green) has converged to the final value. As such, the algorithm becomes certain of the correct label (in this case, "Up"). In this sense, NeuralThink is able to learn how to solve a complex maze-solving algorithm by predicting the next immediate step of the agent. This results highlight the strong connection between propagation of information in the model and the final learned algorithm. We provide more examples of learned algorithms in Appendix H.

3.3. Implementation details

Precomputation of States We provide the original observation as input to recurrent convolutional block at every iteration. For computational efficiency, we precompute the input observation operation on the first iteration and store it for subsequent iterations. A pseudo-code implementation of this optimization is in Appendix B.1.

Model Checkpoint Selection For training we consider a training and validation set split of 80% and 20%, respectively. To select the model checkpoint to be used for evaluation, we consider the one that has the best performance on the validation set. In case of ties due to similar performance, we select the later model checkpoint.

Training Loss The benchmarks we use are considered classification problems and as such we train our models using cross-entropy loss. In asymmetrical tasks, this approach resembles typical behavior cloning, allowing us to apply our learned algorithm directly in sequential decision-making problems, as we show in Section 5.4.

4. Evaluation

We evaluate NeuralThink in regards to the ability to learn to perform tasks over small-size inputs and extrapolate, i.e., executing the same task over larger input sizes without further training. We use symmetrical and asymmetrical tasks as evaluation scenarios, detailed in Section 4.1, and compare the proposed NeuralThink with the baselines described in Section 4.2.

Table 1: Extrapolation accuracy results on the symmetrical tasks benchmark proposed in (Schwarzschild et al., 2021) and the Thin-Maze environment, with training and evaluation sizes (s_t, s_T) shown in the Table. Higher is better. All results are averaged over 10 randomly-selected seeds. We highlight the best average results. We use a (\dagger) to indicate stochastic dominance ($\epsilon_{\min} = 0$) and a (*) to indicate almost stochastic dominance ($\epsilon_{\min} < 0.5$) of NeuralThink over the baseline. We evaluate DeepThink trained with progressive loss (PL) and without it. NeuralThink outperforms the baselines, being able to consistently extrapolate to larger environments.

Model	Prefix-Sum (32, 512)	Maze (24, 124)	Thin-Maze (11, 61)	Chess (8, 8)
NeuralThink (Ours)	100.00 ± 0.00	100.00 ± 0.00	99.97 ± 0.09	84.30 ± 0.40
DeepThink	99.78 $\pm 0.78^*$	86.63 $\pm 28.21^*$	46.78 $\pm 37.49 \dagger$	79.99 $\pm 3.27 \dagger$
DeepThink + PL	100.00 $\pm 0.01^*$	91.13 $\pm 27.37^*$	42.76 $\pm 37.56 \dagger$	82.96 $\pm 0.19 \dagger$
FeedForward	0.00 $\pm 0.00 \dagger$	0.00 $\pm 0.00 \dagger$	0.00 $\pm 0.00 \dagger$	76.95 $\pm 0.35 \dagger$

4.1. Scenarios

For symmetrical tasks, we use the benchmark recently proposed by (Schwarzschild et al., 2021), consisting of three tasks: a binary task (Prefix-Sum), a maze-solving task (Maze), and a chess puzzle task (Chess). Additionally, we modify the Maze task to allow smaller size inputs, which we denote by Thin-Maze. For a detailed description of these tasks, we refer the reader to the original paper.

Given the absence of a benchmark for extrapolation with asymmetrical tasks, we contribute four new scenarios, depicted in Fig. 4. These new scenarios consider as input images of arbitrary sizes and as output vectors of fixed dimensions (more details in Appendix A):

GoTo: Inspired by the Minigrid environment (Chevalier-Boisvert et al., 2023), the goal of the task is to select the action that moves the agent closer to the exit position. As shown in Fig. 4a the input is an image observation of an environment with arbitrary size that contains the player and goal positions. The output of this task is a four-dimensional one-hot vector, corresponding to the actions available to the agent (up, down, left, right).

1S-Maze: Inspired by the Maze environment from the symmetrical task benchmark, the objective of the task is to select the action that moves the agent closer to the goal position. As shown in Fig. 4b the input is an image observation of a maze with arbitrary size, containing the player and goal positions. The output of this task is a four-dimensional one-hot vector, corresponding to the actions available to the agent (up, down, left, right).

Pong: Inspired by the Atari Pong game, as seen in Fig. 4c, the goal of the task is to select the action that moves the paddle horizontally to be underneath the ball. The input is an image observation of the game with arbitrary size that contains the player (paddle) and the ball positions, as seen in Fig. 4c. The output of this task is a three-dimensional

one-hot vector, corresponding to the actions available to the agent (left, right, no action).

Doorkey: Inspired by the Doorkey environment in Mini-grid (Chevalier-Boisvert et al., 2023), the goal of this multi-step task is to reach the goal position (red pixel on bottom right) by first picking-up a key and using it to open a lock door. As shown in Fig. 4d, the input is an image observation of the environment with arbitrary size that contains the player, key, door and goal positions. The output is a four-dimensional one-hot vector, corresponding to the actions available to the agent (forward, rotate right, grab, toggle).

4.2. Baselines

DeepThink (Bansal et al., 2022) The current state-of-the-art Deep Thinking architecture, that combines a recurrent Resnet network, with a recall module and progressive loss. We employ the original source code from the authors and suggested training hyperparameters (when available).

FeedForward A non-recurrent feed-forward network, based on the ResNet architecture, that has a fixed number of layers. This baseline is used to show the importance of the recurrent module for extrapolation.

Random A lower-bound baseline, that randomly samples a random output. This model is used to help understand the worst-case performance of the models in asymmetrical tasks.

As the baseline models cannot be applied directly in asymmetrical tasks, we modify them by introducing a global pooling layer, following our architecture. In Appendix B we present a complete description of the baselines.

4.3. Statistical significance

We compare NeuralThink against the baselines through the Almost Stochastic Order (ASO) test for statistical signifi-

Table 2: Extrapolation accuracy results on the asymmetrical tasks benchmark, with training and evaluation sizes (s_t, s_T) shown in the Table. We employ curriculum learning to train all methods, with training observation sizes indicated in the Table. Higher is better. We highlight the best average results. We use a (\dagger) to indicate stochastic dominance ($\epsilon_{\min} = 0$) of NeuralThink. All results are averaged over 10 randomly-selected seeds. NeuralThink significantly outperforms the baselines, being able to consistently extrapolate to larger environments.

Model	GoTo ([6, 20], 128)	1S-Maze ([5, 13]], 121)	Pong ([6, 20], 128)	DoorKey ([6, 20], 128)
NeuralThink (Ours)	100.00 ± 0.00	100.00 ± 0.00	100.00 ± 0.00	100.00 ± 0.00
DeepThink	75.92 ± 2.26 \dagger	64.32 ± 8.86 \dagger	71.97 ± 10.70 \dagger	97.13 ± 1.46 \dagger
FeedForward	73.00 ± 0.55 \dagger	56.82 ± 3.74 \dagger	48.99 ± 11.25 \dagger	79.22 ± 11.86 \dagger
Random	29.90 ± 0.18 \dagger	29.46 ± 0.40 \dagger	37.87 ± 0.47 \dagger	29.52 ± 0.58 \dagger

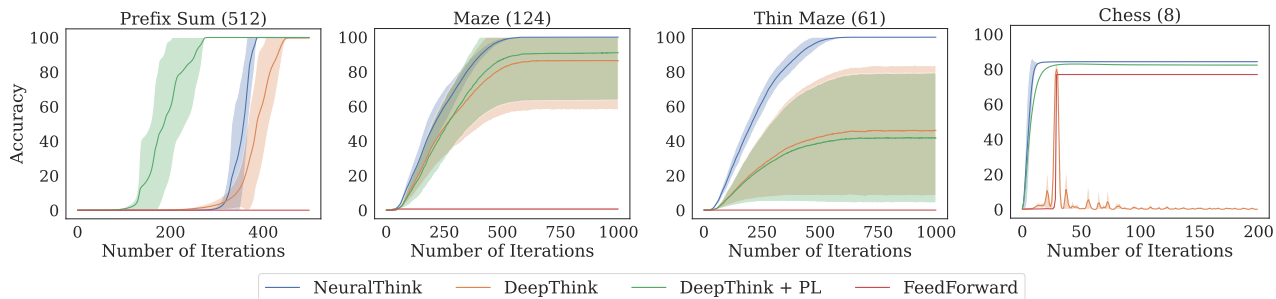


Figure 5: Extrapolation accuracy of the different methods as a function of the number of iterations in the symmetrical task benchmark. All results are averaged over 10 randomly-selected seeds. The results show that NeuralThink provides more stable extrapolation (with less variance than the baselines) without suffering from overthinking.

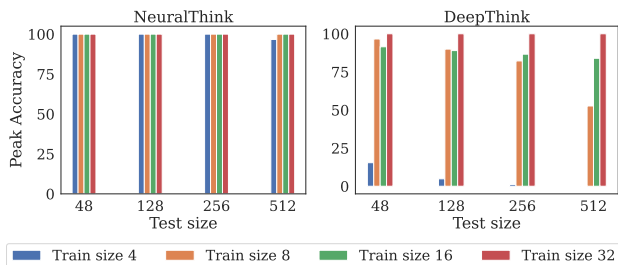


Figure 6: Accuracy of extrapolation to large input sizes in Prefix-Sum. Higher is better. NeuralThink is able to extrapolate consistently from smaller training sizes, thus requiring less computational resources during training.

cance (Dror et al., 2019; Del Barrio et al., 2018). All tests use a significance level of $\alpha = 0.05$ and employ the Bonferroni correction (Bonferroni, 1936) for multiple comparisons. For more details on the ASO test and the statistical significance results, we refer the reader to Appendix G.

5. Results

We start by considering symmetrical tasks and show that our architecture outperforms prior state-of-the-art Deep Think-

ing approaches, as shown in Section 5.1. In Section 5.2, we consider asymmetrical tasks and show that NeuralThink can extrapolate to arbitrarily large sizes without a significant loss in performance. We perform an ablation study of NeuralThink in Section 5.3 that highlights the role of all components in our architecture for extrapolation. Finally, in Section 5.4 we highlight how our method can be directly applied to solve visual sequential decision-making tasks by using the learned algorithm as a policy in a reinforcement learning scenario where, at execution time, the agent is provided with images of arbitrary size.

5.1. Symmetrical Tasks

We start by evaluating the extrapolation performance of NeuralThink against the baselines in the symmetrical benchmark tasks (Schwarzschild et al., 2021), presenting the results in Table 1.

NeuralThink achieves state-of-the-art extrapolation performance on symmetrical tasks. In particular, our approach is able to achieve a 100% accuracy on the Prefix-Sum and Maze tasks, when evaluated on a scenario with observations 16 and 5 times bigger, respectively, than during training. On the more complex Chess task, our model

Table 3: Extrapolation accuracy of different versions of NeuralThink in the proposed asymmetrical tasks. Higher is better. We highlight the best average results. We use a (†) to indicate stochastic dominance ($\epsilon_{\min} = 0$) and a (*) to indicate almost stochastic dominance ($\epsilon_{\min} < 0.5$) of NeuralThink over the baseline. All results are averaged over 10 randomly-selected seeds. The results show that removing each component of NeuralThink results in a decrease in performance of our method.

Ablation Component	GoTo	1S-Maze	Pong	DoorKey
NeuralThink	100.00 ± 0.00	100.00 ± 0.00	100.00 ± 0.00	100.00 ± 0.00
Use AvgPool	90.42 ± 22.31 †	97.00 ± 3.87 †	92.86 ± 14.66 †	51.86 ± 38.98 †
Use 5L	79.77 ± 4.69 †	84.16 ± 16.39 †	100.00 ± 0.00	92.99 ± 7.62 †
No Curriculum Learning	95.47 ± 7.19 †	64.12 ± 23.50 †	100.00 ± 0.00	97.23 ± 4.73 *
No LSTM	81.63 ± 10.02 †	67.28 ± 14.51 †	76.12 ± 17.63 †	93.68 ± 7.88 †

still outperforms the other baselines, achieving an average accuracy of 84.30%.

To understand what is the minimal input size during training required to achieve a good extrapolation performance, we perform a study on the `Prefix-Sum` environment. In Figure 6 we show the performance of our model with different training sizes. The results show that NeuralThink is able to extrapolate when provided with smaller input observations during training, in comparison with the previous state-of-the-art. In particular, NeuralThink is able to successfully extrapolate to large observations (e.g., 512-dimensional) when provided with small observations (e.g., 8-dimensional).

NeuralThink also does not suffer from the overthinking problem without the use of Progressive Loss, as seen in Figure 5.

5.2. Asymmetrical Tasks

We now evaluate the extrapolation performance of NeuralThink against the baselines in the asymmetrical tasks and present the results in Table 2.

The results show that NeuralThink surpasses previous state-of-the-art in allowing extrapolation in asymmetrical tasks. In particular, our approach is able to achieve perfect accuracy when extrapolating to observation sizes 9 (`1S-Maze`) and 6 (`GoTo`, `Pong`, `DoorKey`) times larger than the ones provided during training.

Additionally, we explore the setting of *extreme* extrapolation and evaluate our model on very large image sizes (256, 512). As shown in Figure 7, even in such challenging conditions NeuralThink is able to consistently extrapolate without losing performance, while the baseline fails to do so.

5.3. Ablation Study

We perform an ablation study on the components of NeuralThink and present them in Table 3. In particular, we evaluate the role of: (i) the aggregation function (use AvgPool), (ii)

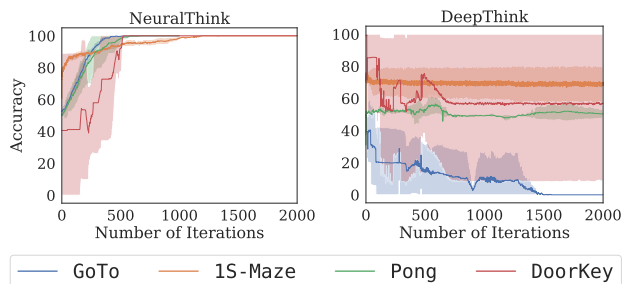


Figure 7: Accuracy results of extrapolation to large observation sizes (512×512). All results are averaged over 10 randomly-selected seeds. In the `1S-Maze` environment, the real number of iterations is 10x larger. Higher is better. NeuralThink is the only model able to extrapolate in these challenging conditions.

the depth of recurrent convolutional block (use 5L), (iii) the training method (no curriculum learning) and (iv) the type of recurrent layer in the convolutional block (no LSTM).

The results show that every component of NeuralThink contributes to the overall extrapolation performance of the method. In particular, the use of an LSTM layer instead of a ResNet block in the recurrent convolutional block results in a significant improvement in performance. This result is aligned with previous works that have shown that gated-based recurrent neural networks empirically learn and generalize better than recurrent ResNets (Price et al., 2016). The use of max pooling as the aggregation function results in better performance than average pooling. Removing curriculum learning also results in a decrease in extrapolation performance of the method in some tasks (e.g., navigation), highlighting the need to consider multiple (small) image sizes to extract relevant information during the training procedure. We also observe a performance gain in using a single convolutional layer over a block of five layers (as used in (Bansal et al., 2022)), despite requiring five times more the number of iterations to compensate. Finally, we

Table 4: Average reward returns on the Minigrid Doorkey environment, with different sizes during execution. We show the average reward multiplied by 10^2 . We employ curriculum learning to train all methods. Higher is better. We highlight the best average results. We use a (\dagger) to indicate stochastic dominance ($\epsilon_{\min} = 0$) and a (*) to indicate almost stochastic dominance ($\epsilon_{\min} < 0.5$) of NeuralThink over the baseline. All results are averaged over 10 randomly-selected seeds. NeuralThink significantly outperforms the baselines, being able to consistently extrapolate to larger observations without loss of performance.

Model	8×8	20×20	32×32	64×64	128×128
Oracle	97.00 ±0.05	98.92 ±0.02	99.35 ±0.01	99.69 ±0.00	99.85 ±0.00
NeuralThink (Ours)	96.24 ±1.29	98.82 ±0.26	99.12 ±0.57	98.69 ±2.44	98.02 ±2.54
DeepThink	95.49 ±1.81 *	98.47 ±0.48 *	91.41 ±10.64 †	43.09 ±31.18 †	24.71 ±31.76 †
FeedForward	95.91 ±2.58	96.14 ±1.63 †	63.51 ±7.63 †	23.53 ±7.34 †	7.19 ±3.18 †

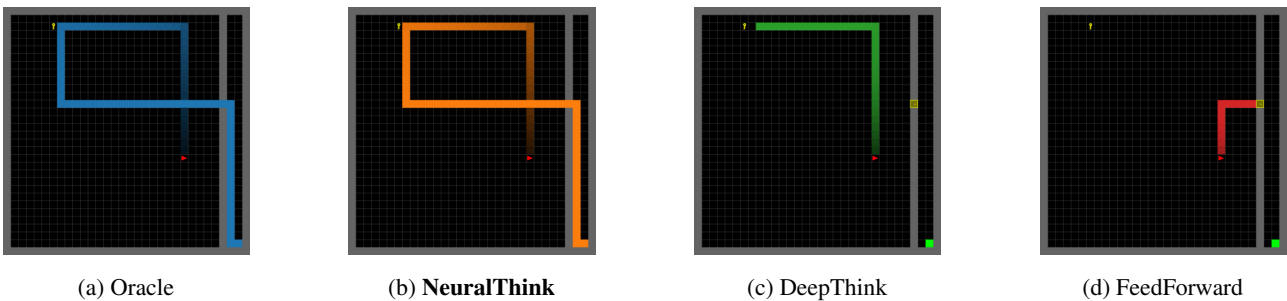


Figure 8: Example trajectories of the different methods when extrapolating to a Minigrid Doorkey environment with an image observation of size 64×64 . The trajectory of the agents follows the gradient of the line (from darker to brighter). The results show that only NeuralThink is able to follow the oracle police. Additional examples in Appendix I.

also note that empirically we found that removing the LSTM component of NeuralThink often results in unstable training.

5.4. Extrapolation on Sequential Decision-Making Tasks

To highlight the versatility of NeuralThink, we now consider visual sequential decision-making problems, in which, at each time-step, the algorithm is provided with an image of arbitrary size, and needs to output an action. The challenge of these tasks resides in the fact that they can only be solved by selecting a correct sequence of actions, and, thus, small errors can quickly accumulate and lead to a wrong solution.

We once again consider the DoorKey environment and train NeuralThink using a dataset collected by a pretrained oracle policy. Subsequently, we employ the learned algorithm in the Minigrid DoorKey environment (Chevalier-Boisvert et al., 2023), directly as the agent’s policy: at each time-step, mapping the observations of the agent (images of arbitrary size) into actions. We evaluate the performance of our method in extrapolating at execution time to larger observations against oracle policies specifically trained on each observation size.

The results in Table 4 highlight how NeuralThink can

achieve oracle-level performances in settings with larger observation sizes despite *never being trained on such conditions*. Moreover, the prior baselines struggle to maintain their performance for larger observations due to the accumulation of errors during task-execution, resulting in sub-optimal trajectories as shown in Figure 8.

6. Conclusion

We proposed NeuralThink, a simple architecture that learns algorithms that can perform extrapolation across general tasks. We showed that our architecture consistently outperforms prior state-of-the-art Deep Thinking networks in regards to extrapolation from small training observations to large observations at test time. In future work, we plan on exploring the merging of NeuralThink with reinforcement learning approaches in order to learn to perform sequential decision-making tasks in an online manner, while maintaining the ability to extrapolate.

Ethical Statement

This work endows machine learning methods to achieve better and new extrapolation abilities across tasks with equal

and different input and output sizes. As such, this work does not have direct ethical implications.

Acknowledgements

This work was partially supported by national funds through Fundação para a Ciência e a Tecnologia (FCT) with ref. UIDB/50021/2020 and the project RELEvaNT, ref. PTDC/CCI-COM/5060/2021. The first author acknowledges the FCT PhD grant 2023.02298.BD. This work has also been supported by the Swedish Research Council, Knut and Alice Wallenberg Foundation and the European Research Council (ERC-BIRD).

References

- Ba, L. J., Kiros, J. R., and Hinton, G. E. Layer normalization. *CoRR*, abs/1607.06450, 2016. doi: 10.48550/arxiv.1607.06450.
- Bansal, A., Schwarzschild, A., Borgnia, E., Emam, Z., Huang, F., Goldblum, M., and Goldstein, T. End-to-end algorithm synthesis with recurrent networks: Extrapolation without overthinking. In *NeurIPS, 2022*.
- Bevilacqua, B., Nikiforou, K., Ibarz, B., Bica, I., Paganini, M., Blundell, C., Mitrovic, J., and Velickovic, P. Neural algorithmic reasoning with causal regularisation. In Krause, A., Brunskill, E., Cho, K., Engelhardt, B., Sabato, S., and Scarlett, J. (eds.), *International Conference on Machine Learning, ICML 2023, 23-29 July 2023, Honolulu, Hawaii, USA*, volume 202 of *Proceedings of Machine Learning Research*, pp. 2272–2288. PMLR, 2023.
- Bonferroni, C. *Teoria statistica delle classi e calcolo delle probabilità*. Pubblicazioni del R. Istituto superiore di scienze economiche e commerciali di Firenze. Seeber, 1936.
- Chevalier-Boisvert, M., Dai, B., Towers, M., de Lazcano, R., Willems, L., Lahlou, S., Pal, S., Castro, P. S., and Terry, J. Minigrid & miniworld: Modular & customizable reinforcement learning environments for goal-oriented tasks. *CoRR*, abs/2306.13831, 2023.
- Dehghani, M., Gouws, S., Vinyals, O., Uszkoreit, J., and Kaiser, L. Universal transformers. In *7th International Conference on Learning Representations, ICLR 2019, New Orleans, LA, USA, May 6-9, 2019*. OpenReview.net, 2019.
- Del Barrio, E., Cuesta-Albertos, J. A., and Matrán, C. An optimal transportation approach for assessing almost stochastic order. *The Mathematics of the Uncertain: A Tribute to Pedro Gil*, pp. 33–44, 2018.
- Dror, R., Shlomov, S., and Reichart, R. Deep dominance - how to properly compare deep neural models. In Korhonen, A., Traum, D. R., and Màrquez, L. (eds.), *Proceedings of the 57th Conference of the Association for Computational Linguistics, ACL 2019, Florence, Italy, July 28- August 2, 2019, Volume 1: Long Papers*, pp. 2773–2785. Association for Computational Linguistics, 2019. doi: 10.18653/V1/P19-1266.
- Elbayad, M., Gu, J., Grave, E., and Auli, M. Depth-adaptive transformer. In *8th International Conference on Learning Representations, ICLR 2020, Addis Ababa, Ethiopia, April 26-30, 2020*. OpenReview.net, 2020.
- Eyzaguirre, C. and Soto, Á. Differentiable adaptive computation time for visual reasoning. In *2020 IEEE/CVF Conference on Computer Vision and Pattern Recognition, CVPR 2020, Seattle, WA, USA, June 13-19, 2020*, pp. 12814–12822. Computer Vision Foundation / IEEE, 2020. doi: 10.1109/CVPR42600.2020.01283.
- Freivalds, K. and Liepins, R. Improving the neural GPU architecture for algorithm learning. *CoRR*, abs/1702.08727, 2017. doi: 10.48550/arxiv.1702.08727.
- Graves, A. Adaptive computation time for recurrent neural networks. *CoRR*, abs/1603.08983, 2016. doi: 10.48550/arxiv.1603.08983.
- Graves, A., Wayne, G., and Danihelka, I. Neural Turing machines. *CoRR*, abs/1410.5401, 2014. doi: 10.48550/arxiv.1410.5401.
- He, K., Zhang, X., Ren, S., and Sun, J. Delving deep into rectifiers: Surpassing human-level performance on imagenet classification. In *2015 IEEE International Conference on Computer Vision, ICCV 2015, Santiago, Chile, December 7-13, 2015*, pp. 1026–1034. IEEE Computer Society, 2015. doi: 10.1109/ICCV.2015.123.
- He, K., Zhang, X., Ren, S., and Sun, J. Deep residual learning for image recognition. In *Proceedings of the IEEE conference on computer vision and pattern recognition*, pp. 770–778, 2016.
- Ibarz, B., Kurin, V., Papamakarios, G., Nikiforou, K., Benani, M., Csordás, R., Dudzik, A. J., Bosnjak, M., Vitvitskyi, A., Rubanova, Y., Deac, A., Bevilacqua, B., Ganin, Y., Blundell, C., and Velickovic, P. A generalist neural algorithmic learner. In Rieck, B. and Pascanu, R. (eds.), *Learning on Graphs Conference, LoG 2022, 9-12 December 2022, Virtual Event*, volume 198 of *Proceedings of Machine Learning Research*, pp. 2. PMLR, 2022.
- Jumper, J., Evans, R., Pritzel, A., Green, T., Figurnov, M., Ronneberger, O., Tunyasuvunakool, K., Bates, R., Žídek, A., Potapenko, A., et al. Highly accurate protein structure

- prediction with alphafold. *Nature*, 596(7873):583–589, 2021.
- Kaiser, L. and Sutskever, I. Neural gpus learn algorithms. In Bengio, Y. and LeCun, Y. (eds.), *4th International Conference on Learning Representations, ICLR 2016, San Juan, Puerto Rico, May 2-4, 2016, Conference Track Proceedings*, 2016.
- Mnih, V., Kavukcuoglu, K., Silver, D., Graves, A., Antonoglou, I., Wierstra, D., and Riedmiller, M. Playing Atari with deep reinforcement learning. *CoRR*, abs/1312.5602, 2013.
- Price, E., Zaremba, W., and Sutskever, I. Extensions and limitations of the neural GPU. *CoRR*, abs/1611.00736, 2016. doi: 10.48550/arxiv.1611.00736.
- Salle, A. and Malmasi, S. A simple loss function for convergent algorithm synthesis using rnns. In Maughan, K., Liu, R., and Burns, T. F. (eds.), *The First Tiny Papers Track at ICLR 2023, Tiny Papers @ ICLR 2023, Kigali, Rwanda, May 5, 2023*. OpenReview.net, 2023.
- Salle, A. and Prates, M. O. R. Think again networks and the delta loss. *CoRR*, abs/1904.11816, 2019.
- Schmidhuber, J. Self-delimiting neural networks. *CoRR*, abs/1210.0118, 2012. doi: 10.48550/arxiv.1210.0118.
- Schwarzschild, A., Borgnia, E., Gupta, A., Huang, F., Vishkin, U., Goldblum, M., and Goldstein, T. Can you learn an algorithm? generalizing from easy to hard problems with recurrent networks. In Ranzato, M., Beygelzimer, A., Dauphin, Y. N., Liang, P., and Vaughan, J. W. (eds.), *Advances in Neural Information Processing Systems 34: Annual Conference on Neural Information Processing Systems 2021, NeurIPS 2021, December 6-14, 2021, virtual*, pp. 6695–6706, 2021.
- Shi, X., Chen, Z., Wang, H., Yeung, D., Wong, W., and Woo, W. Convolutional LSTM network: A machine learning approach for precipitation nowcasting. In Cortes, C., Lawrence, N. D., Lee, D. D., Sugiyama, M., and Garnett, R. (eds.), *Advances in Neural Information Processing Systems 28: Annual Conference on Neural Information Processing Systems 2015, December 7-12, 2015, Montreal, Quebec, Canada*, pp. 802–810, 2015.
- Trask, A., Hill, F., Reed, S. E., Rae, J. W., Dyer, C., and Blunsom, P. Neural arithmetic logic units. In Bengio, S., Wallach, H. M., Larochelle, H., Grauman, K., Cesa-Bianchi, N., and Garnett, R. (eds.), *Advances in Neural Information Processing Systems 31: Annual Conference on Neural Information Processing Systems 2018, NeurIPS 2018, December 3-8, 2018, Montréal, Canada*, pp. 8046–8055, 2018.
- Ulmer, D., Hardmeier, C., and Frellsen, J. deep-significance - easy and meaningful statistical significance testing in the age of neural networks. *CoRR*, abs/2204.06815, 2022. doi: 10.48550/ARXIV.2204.06815.
- Velickovic, P., Badia, A. P., Budden, D., Pascanu, R., Bano, A., Dashevskiy, M., Hadsell, R., and Blundell, C. The CLRS algorithmic reasoning benchmark. In Chaudhuri, K., Jegelka, S., Song, L., Szepesvári, C., Niu, G., and Sabato, S. (eds.), *International Conference on Machine Learning, ICML 2022, 17-23 July 2022, Baltimore, Maryland, USA*, volume 162 of *Proceedings of Machine Learning Research*, pp. 22084–22102. PMLR, 2022.
- Zaremba, W. and Sutskever, I. Learning to execute. *CoRR*, abs/1410.4615, 2014. doi: 10.48550/arxiv.1410.4615.
- Zaremba, W. and Sutskever, I. Reinforcement learning neural turing machines. *CoRR*, abs/1505.00521, 2015. doi: 10.48550/arxiv.1505.00521.

A. Datasets Technical Details

A.1. Assymetrical Tasks

To build the datasets, we followed a consistent approach across all tasks. Each dataset consists of 50,000 training examples, with 80% used for training and 20% for validation. Additionally, we included 10,000 test examples for evaluation purposes, with a bigger size than the training examples.

A.1.1. GoTo

Inspired by the Minigrid Environment (Chevalier-Boisvert et al., 2023), the GoTo task is a simple grid setting, with a 1-pixel white border, and 1-pixel green player, and a 1-pixel red goal, as seen in Fig. 4a. The player has 4 actions (up, down, left, right) available. To generate the dataset we use a simple path-finding algorithm from the player to the goal, where the agent starts by minimizing the vertical distance to the goal until it reaches the same vertical position, and then minimizes the horizontal distance until it reaches the goal.

A.1.2. 1S-MAZE

This task is based on the maze task from (Schwarzschild et al., 2021) and is used on the symmetrical task evaluation. The input is a maze with the player and goal positions, and the objective is to move the player (in green) to the goal (in red) position by solving the maze. We use the official dataset from the original paper, where we made the green player have a random start position so that it does not become trivial to solve. We also changed the thickness of the walls and the border to 1 pixel, as seen in Fig. 4b. The outputs are 4 actions (up, down, left, right). The dataset is generated using a depth-first search algorithm, where the label is the next action to take to reach the goal.

A.1.3. PONG

Using the Atari Pong game as inspiration, the pong task is a simplified version of the game, where the objective is to move the paddle to the ball position, as seen in Fig. 4c. To solve this task, the player has 3 actions (left, right, stay) available. The dataset is generated by a simple agent that follows the ball, keeping the paddle centered on the ball.

A.1.4. DOORKEY

This task uses the Minigrid Doorkey environment from (Chevalier-Boisvert et al., 2023), where the objective is to move the player (red pixel on top) to the goal (red pixel on bottom right), by first moving to the key (yellowish pixel), grabbing it, and then moving to the door (different color pixel on middle separator) and opening it and finally moving to the goal, as seen in Fig. 4d. For the dataset, we simplify the original action space to 4 actions (forward, rotate right, grab, toggle), and generate labels using a simple oracle agent that solves the task.

The original reinforcement learning environment receives a reward of $1 - 0.9 * (step_count / max_steps)$ if the agent reaches the goal in $step_count$ steps, and 0 otherwise. In conjunction with the oracle agent, we use this environment to evaluate the performance of the learned algorithm in the original environment.

To evaluate the environments faster we parallelize the environments, however naively parallelizing the environments leads to bias in the results, thus we make sure that if we start an episode we always end it. To speed up the evaluation we also made a simple cycle check on the environment. The agent is deterministic, thus if the agent is in the same state, the output action will be the same. Therefore if the agent visits the same state, it means that it is in a cycle, and we terminate the environment with reward 0.

A.2. Symmetrical Tasks

To show that our new model also is able to extrapolate on symmetrical tasks, we evaluate our method on the benchmark presented in (Schwarzschild et al., 2021).

Both the prefix sum and maze tasks use 50,000 training examples, with 80% used for training and 20% for validation, and 10,000 test examples for evaluation purposes. On the other hand, the chess task uses 600,000 training examples and 100,000 test examples. Here we present a short description of the tasks used in the benchmark, for a more detailed description please refer to the original paper.

A.2.1. PREFIX-SUM

The prefix sums task consists of computing the prefix-sum modulo two of an input binary array, where the i_n bit of the output is the modulo two sum of the current and the previous n bits of the input.

A.2.2. MAZE

The maze task is a maze-solving task where the output is the path from the player to the goal.

The training is done on mazes of size 24×24 pixels, and tested on mazes of size 124×124 . While on the original paper, it is referred that the mazes have a training size of 9 and a test size of 59, each maze has a border of 3 pixels and the paths have a width of 2 pixels, thus $9 * 2 + 3 * 2 = 24$ and $59 * 2 + 3 * 2 = 124$.

A.2.3. THIN-MAZE

Similar to the 1S-Maze task, this task uses the maze code from (Schwarzschild et al., 2021), and changes the thickness of the walls and the border to 1 pixel. Thus the training and test sizes are 11×11 and 61×61 , respectively.

A.2.4. CHESS

The chess task comprises of chess puzzles, where the input is an $8 \times 8 \times 12$ array indicating the position of the pieces on the board, and the output is an 8×8 binary array indicating the optimal move origin and position to solve the puzzle. Using the original dataset, the training involves 600,000 puzzles below a rating of 1,385, while testing employs 100,000 examples above this threshold.

A.3. Training Details

In Table 5 we show the training and test sizes for each task, as well as the number of training and test examples. The sizes of the tasks used in the curriculum learning are inside brackets. The biggest size in the brackets is the one used for validation.

Task	Train size	Test Size	Training examples	Test examples
GoTo	[6,8,10,12,15,17,20]	128	50,000	10,000
1S-Maze	[5,7,9,11,13]	121	50,000	10,000
Pong	[6,8,10,12,15,17,20]	128	50,000	10,000
Doorkey	[6,8,10,12,15,17,20]	128	50,000	10,000
Prefix-Sum	32	512	50,000	10,000
Maze	24	124	50,000	10,000
Thin-Maze	11	61	50,000	10,000
Chess	8	8	600,000	100,000

Table 5: Dataset specifications. The training sizes inside brackets are the sizes used for curriculum learning.

B. Architecture

The structures employed in our experiments with the exception of NeuralThink closely resemble those outlined by (Schwarzschild et al., 2021; Bansal et al., 2022). We present the specific details here for convenience.

In all models, we have a convolutional layer with 3×3 filters (or length-three filters in the 1D case), followed by a ReLU non-linearity, which transforms the input into feature space. Each filter advances by one unit, and inputs are padded with one unit in each direction. All convolutional layers in all models use the same length-three filters and padding scheme, without bias terms except for the convolutional layers in the lstm block. The number of filters is defined for each dataset in Table 6 as the "width" of the network. For simplicity, we used the same channel size for all asymmetrical experiments, with the exception of the *output_size* that is dependent on the task.

The recurrent block is a layernorm convolutional lstm as described in Listing 1. In our lstm model, we use a width that is 4 times smaller than the width of the other models to have a comparable number of parameters between the models, since the lstm block uses 4 convolutions. The concluding block consists of three convolutional layers with diminishing widths

(specific values are detailed in Table 1), with ReLUs applied after the first two layers. The last convolutional layer produces two-channel outputs used for binary pixel classification in the case of the same input and output size tasks, or N channel outputs in the case of fixed output size tasks, where N is the number of possible outputs.

Dataset	Width (NeuralThink)	Width (others)	# Channels in Hidden Layers
Asymmetrical Tasks	64	256	64, 64, output_size
Prefix Sum	100	400	400, 200, 2
Maze	32	128	32, 8, 2
Chess	128	512	32, 8, 2

Table 6: Dataset specifications and architecture details.

B.1. Convolutional LSTM Pseudo-code implementation

A pseudo-code implementation of the Convolutional LSTM is shown in Algorithm 1, where T represents the number of iterations, X is the input tensor, H is the hidden state tensor, C is the cell state tensor, W_X and W_H are the weights of the convolutional layers that include the bias term, `layernorm` is a layer normalization function, `conv` is a convolutional operator, `split` is a function that splits the output of a convolutional layer into 4 parts, and `zeros_init` is a function that initializes the hidden state tensor with zeros.

Algorithm 1 LayerNorm Convolutional LSTM

```

1: Input:  $X$  (input sequence),  $W_X$  (weights for input),  $W_H$  (weights for hidden state)
2: /* Pre-compute input: */
3:  $wx \leftarrow \text{layernorm}(\text{conv}(X, W_X))$ 
4:  $wx_i, wx_f, wx_c, wx_o \leftarrow \text{split}(wx, 4)$ 
5: /* Initialize hidden state: */
6:  $H \leftarrow \text{zeros\_initialization}()$ 
7:  $C \leftarrow \text{zeros\_initialization}()$ 
8: for  $t \leftarrow 1$  to  $T$  do
9:    $wh \leftarrow \text{layernorm}(\text{conv}(H, W_H))$ 
10:   $wh_i, wh_f, wh_c, wh_o \leftarrow \text{split}(wh, 4)$ 
11:   $i \leftarrow \text{sigmoid}(wx_i + wh_i)$ 
12:   $f \leftarrow \text{sigmoid}(wx_f + wh_f)$ 
13:   $o \leftarrow \text{sigmoid}(wx_o + wh_o)$ 
14:   $g \leftarrow \text{tanh}(wx_c + wh_c)$ 
15:   $C \leftarrow \text{layernorm}(f * C + i * g)$ 
16:   $H \leftarrow o * \text{tanh}(C)$ 
17: end for

```

C. Hyperparameters

In Table 7 we present the hyperparameters used for each task. In the symmetrical tasks, we attempted to use the same hyperparameters as in (Bansal et al., 2022), with the exception of the Maze task, where we were not able to achieve good results as in the paper with 50 epochs, so we increased to 150 epochs, keeping the decay schedule at epoch number 100 as present in the source code. The Maze and Thin Maze tasks have the same hyperparameters. We also disabled the warm-up for all our models, since we did not notice any difference in the performance of the model.

We did not perform an extensive hyperparameter search, and as such we used mainly the same hyperparameters across all asymmetrical tasks. The major differences were in the 1S-Maze task and the pong task. In the 1S-Maze we increased the number of epochs to 150 and also increased the number of curriculum epochs to 8 since we had a lower number of tasks for the curriculum learning. For the pong task, we decreased the learning rate to $2.5e-4$, as the models achieved better performance quickly, this could also be related to the fact that the pong task has a smaller output space. We also used a gradient clip of 2, since we noticed that improved the learning stability across all models. And finally, we reduced the regularization of the LSTM in the chess task as we noticed that the task required more capacity to learn the algorithm.

Hyperparameter	1S-Maze	Pong	GoTo	Doorkey	Prefix-Sum	Maze	Chess
Optim.	Adam	Adam	Adam	Adam	Adam	Adam	SGD
Learning Rate	1e-3	2.5e-4	1e-3	1e-3	1e-3	1e-3	1e-2
Decay Schedule	[100]	-	-	-	[60, 100]	[100]	[100, 110]
Decay Factor	0.1	-	-	-	0.01	0.1	0.01
Warm-Up	0	0	0	0	10	10	3
Epochs	150	50	50	50	150	150	120
Clip	2	2	2	2	1.0	-	-
Curriculum Epochs	8	4	4	4	-	-	-
Weight Decay	2e-4	2e-4	2e-4	2e-4	2e-4	2e-4	2e-4
Std Dropout (LSTM)	0.3	0.3	0.3	0.3	0.3	0.3	0
Gal Dropout (LSTM)	0.4	0.4	0.4	0.4	0.4	0.4	0

Table 7: Hyperparameter values for different tasks.

D. Overthink Problem Analysis on Asymmetrical Tasks

We can see that our model is able to extrapolate while maintaining a constant performance, while the (Bansal et al., 2022) model still suffers from the overthinking problem on some tasks. Another interesting observation is that while we attain perfect peak performance on the doorkey task, we can see that the performance wiggles a bit across the different iterations. This phenomenon might be the cause of not attaining perfect performance while executing the model on the environment, since we are always using the last iteration of the model. This is an interesting observation that we leave for future work.

E. Extended Related Work

Adaptive neural networks The study of the amount of computation used depending on the problem has been analyzed in works such as Adaptive Neural Networks (Graves, 2016) and Self-Delimiting Neural Networks (Schmidhuber, 2012), surpassing limitations of classical, fixed computation and RNNs. These models use techniques such as Adaptive Compute Time (ACT, (Graves, 2016)) and halting units to regulate computation, aiming for quicker problem-solving. These ideas have been successfully applied to visual reasoning problems (Eyzaguirre & Soto, 2020) and on natural language processing tasks (Dehghani et al., 2019; Elbayad et al., 2020). However, their performance applied to algorithm learning with problems outside the traditional training domains remains unexplored.

F. Extended Results

For the asymmetrical tasks, here we present the results of the training and validation accuracies of the models in Sections F.1, the fine tuning of the progressive loss parameter of the DeepThink model in Section F.2, and the peak accuracy in testing the trained model in very large size task sizes (256,512) in Section F.3.

F.1. Asymmetrical Tasks Training and Validation Accuracies

In Table 8 and Table 9 we show the training and validation accuracies for the asymmetrical tasks, for the models presented in Table 2. We can see that all models achieve near peak performances during training, and as such we can conclude that the models are being trained correctly.

model	1S-Maze	GoTo	Pong	Doorkey
NeuralThink	99.99 +- 0.00	99.99 +- 0.01	100.00 +- 0.00	99.69 +- 0.03
DeepThink	100.00 +- 0.00	99.99 +- 0.01	100.00 +- 0.00	99.97 +- 0.02
FeedForward	100.00 +- 0.00	100.00 +- 0.00	100.00 +- 0.00	99.85 +- 0.05

Table 8: Peak train accuracies on the asymmetrical tasks.

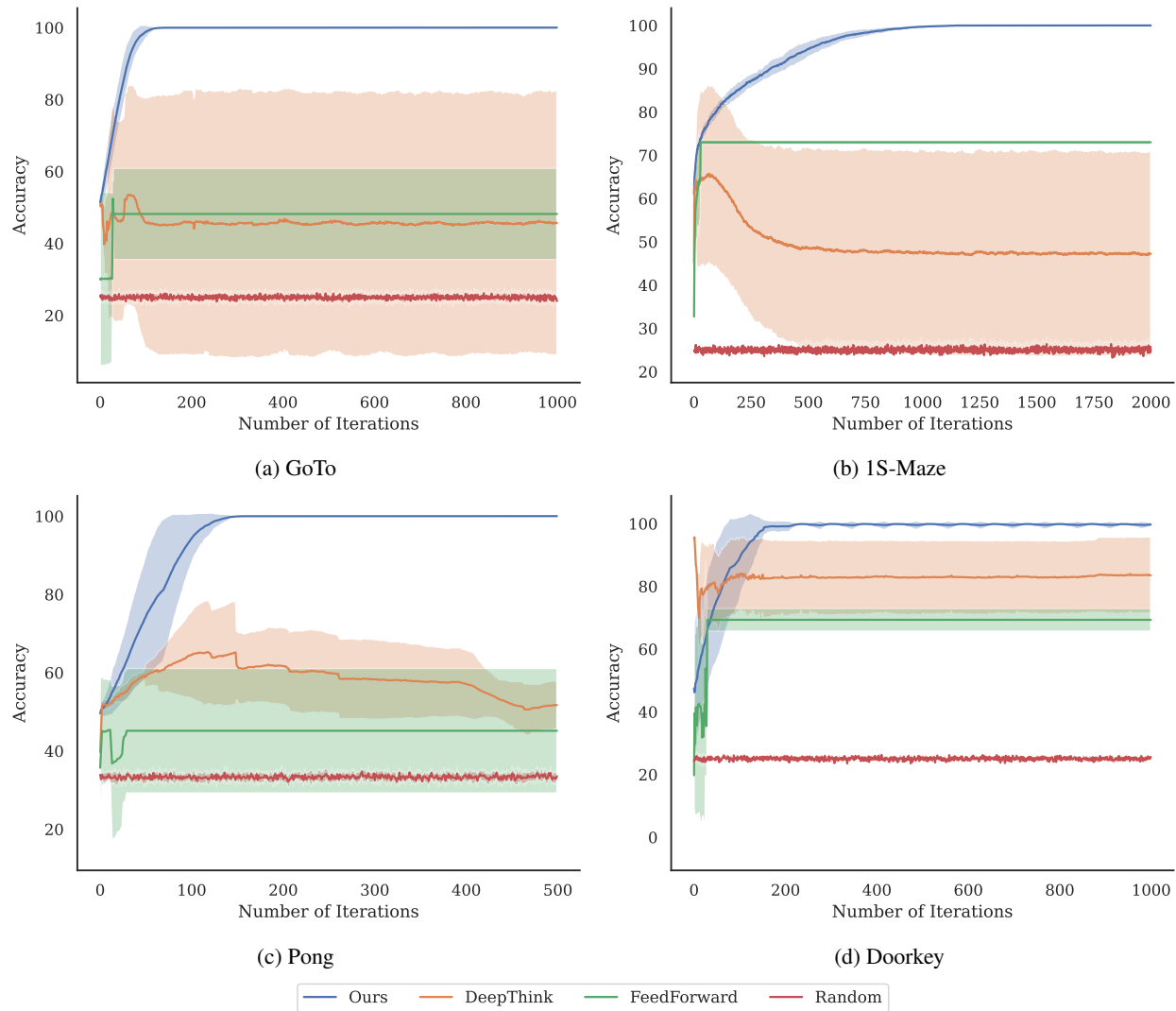


Figure 9: Analysis of the performance of the model on the asymmetrical tasks, as we increase the number of recurrent iterations.

model	1S-Maze	GoTo	Pong	Doorkey
NeuralThink	100.00 +- 0.00	100.00 +- 0.00	100.00 +- 0.00	100.00 +- 0.00
DeepThink	100.00 +- 0.00	100.00 +- 0.00	100.00 +- 0.00	100.00 +- 0.00
FeedForward	100.00 +- 0.00	100.00 +- 0.00	100.00 +- 0.00	99.94 +- 0.04

Table 9: Peak validation accuracies on the asymmetrical tasks.

F.2. Fine-tuning of the Progressive Loss Parameter

The DeepThink (Bansal et al., 2022) model introduces a progressive loss term to help the model extrapolate. However, this term has an alpha parameter that needs to be tuned to each individual task. In Table 10 we show the results of the fine tuning of the alpha parameter for the asymmetrical tasks. For each asymmetrical task we select and present the best-performing alpha value, in bold on Table 2. For the Thin Maze task, we selected both the alpha=0 and the alpha=0.1 for the symmetrical benchmark comparison.

PL alpha value	1S-Maze	GoTo	Pong	Doorkey	Thin Maze
0.00	67.95 +- 6.19	62.98 +- 12.21	69.24 +- 7.60	93.81 +- 6.84	46.78 +- 37.49
0.01	64.99 +- 11.49	64.69 +- 9.23	71.97 +- 10.70	97.13 +- 1.46	42.76 +- 37.56
0.10	74.39 +- 7.44	62.09 +- 13.38	62.53 +- 10.11	93.44 +- 4.71	22.26 +- 27.65
0.50	76.17 +- 1.92	58.45 +- 5.81	68.13 +- 13.27	93.19 +- 8.70	0.22 +- 0.17
1.00	67.80 +- 13.57	60.52 +- 11.75	71.48 +- 14.83	94.71 +- 2.96	5.32 +- 5.84

Table 10: Peak test accuracies for different progressive loss alpha values on the asymmetrical tasks.

F.3. Extreme Extrapolation Results

We also attempted to evaluate the performance of NeuralThink and DeepThink on very large sizes. We tested on sizes 256 and 512, and we show the results in Table 11 and Table 12. Due to the large size of the tasks and the large number of iterations required to solve the tasks, we only tested on 100 examples. Each test on a 1S-Maze task of size 512 took around 28 hours on a 4090 GPU. We can see that NeuralThink is able to maintain perfect accuracy across all tasks.

Test size	1S-Maze	GoTo	Pong	Doorkey
256	100.00 +- 0.00	100.00 +- 0.00	100.00 +- 0.00	100.00 +- 0.00
512	100.00 +- 0.00	100.00 +- 0.00	100.00 +- 0.00	100.00 +- 0.00

Table 11: Peak test accuracies on asymmetrical tasks on very large sizes for the NeuralThink model.

Test size	1S-Maze	GoTo	Pong	Doorkey
256	77.20 +- 2.48	60.33 +- 12.38	65.00 +- 9.01	100.00 +- 0.00
512	79.20 +- 5.81	57.22 +- 10.15	63.60 +- 2.42	99.71 +- 0.45

Table 12: Peak test accuracies on asymmetrical tasks on very large sizes for the DeepThink model.

G. Statistical Significance

The Almost Stochastic Order test (ASO; (Dror et al., 2019; Del Barrio et al., 2018)) was recently introduced to assess statistical significance in Deep Neural Networks across multiple runs. The ASO test measures the presence of a stochastic order between two models or algorithms based on their respective sets of evaluation scores. Using the individual scores of algorithm A and B across various random seeds, the method calculates a test-specific value (ϵ_{\min}), representing how far algorithm A is from being significantly superior to algorithm B. The lower the value of ϵ_{\min} , the more likely it is that A is better than B. For $\epsilon_{\min} < 0.5$, A is said to be *almost stochastically dominant* over B in most cases than vice versa, and thus A could be considered superior to B, although with less confidence. We claim that A is *stochastically dominant* over B with a predefined significance level when $\epsilon_{\min} = 0.0$. We use the implementation by (Ulmer et al., 2022) to perform these statistical tests.

In the following sections, we present the comparison of all pairs of models of the Section 5 and Appendix F.2 each using ASO with a confidence level of $\alpha = 0.05$ (before adjusting for all pair-wise comparisons using the Bonferroni correction (Bonferroni, 1936)).

G.1. Symmetrical Tasks

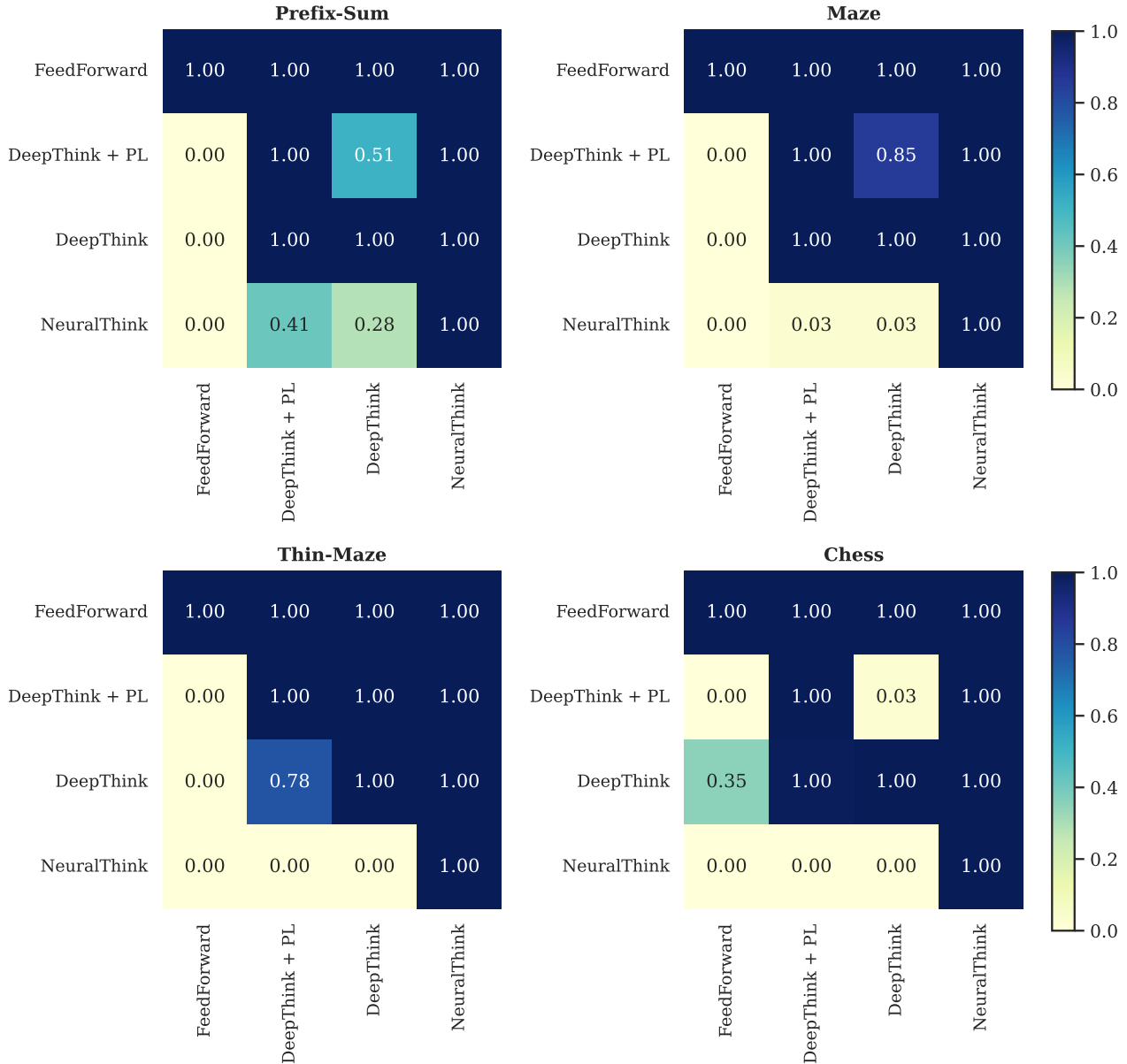


Figure 10: Almost Stochastic Order scores of the symmetrical task results. ASO scores are expressed in ϵ_{\min} , with a significance level $\alpha = 0.05$ that is adjusted accordingly by using the Bonferroni correction (Bonferroni, 1936). Read from row to column: E.g., NeuralThink (row) is almost stochastically dominant over DeepThink (column) in the Prefix-Sum task with ϵ_{\min} of 0.28.

G.2. Assymetrical Tasks

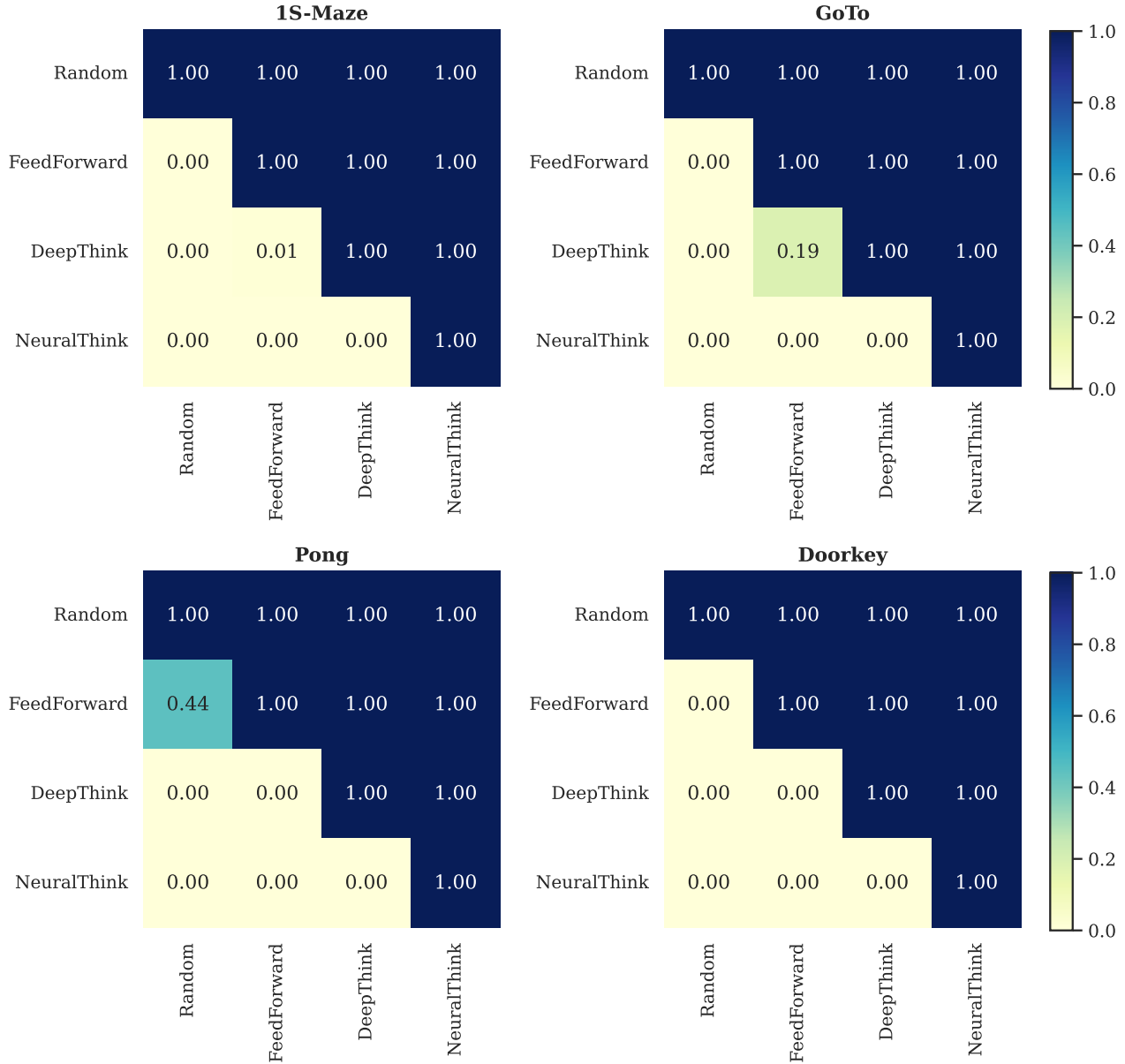


Figure 11: Almost Stochastic Order scores of the assymetrical task results. ASO scores are expressed in ϵ_{\min} , with a significance level $\alpha = 0.05$ that is adjusted accordingly by using the Bonferroni correction (Bonferroni, 1936). Read from row to column: E.g., NeuralThink (row) is stochastically dominant over DeepThink (column) in the 1S-Maze task with ϵ_{\min} of 0.00.

G.3. Ablation Study

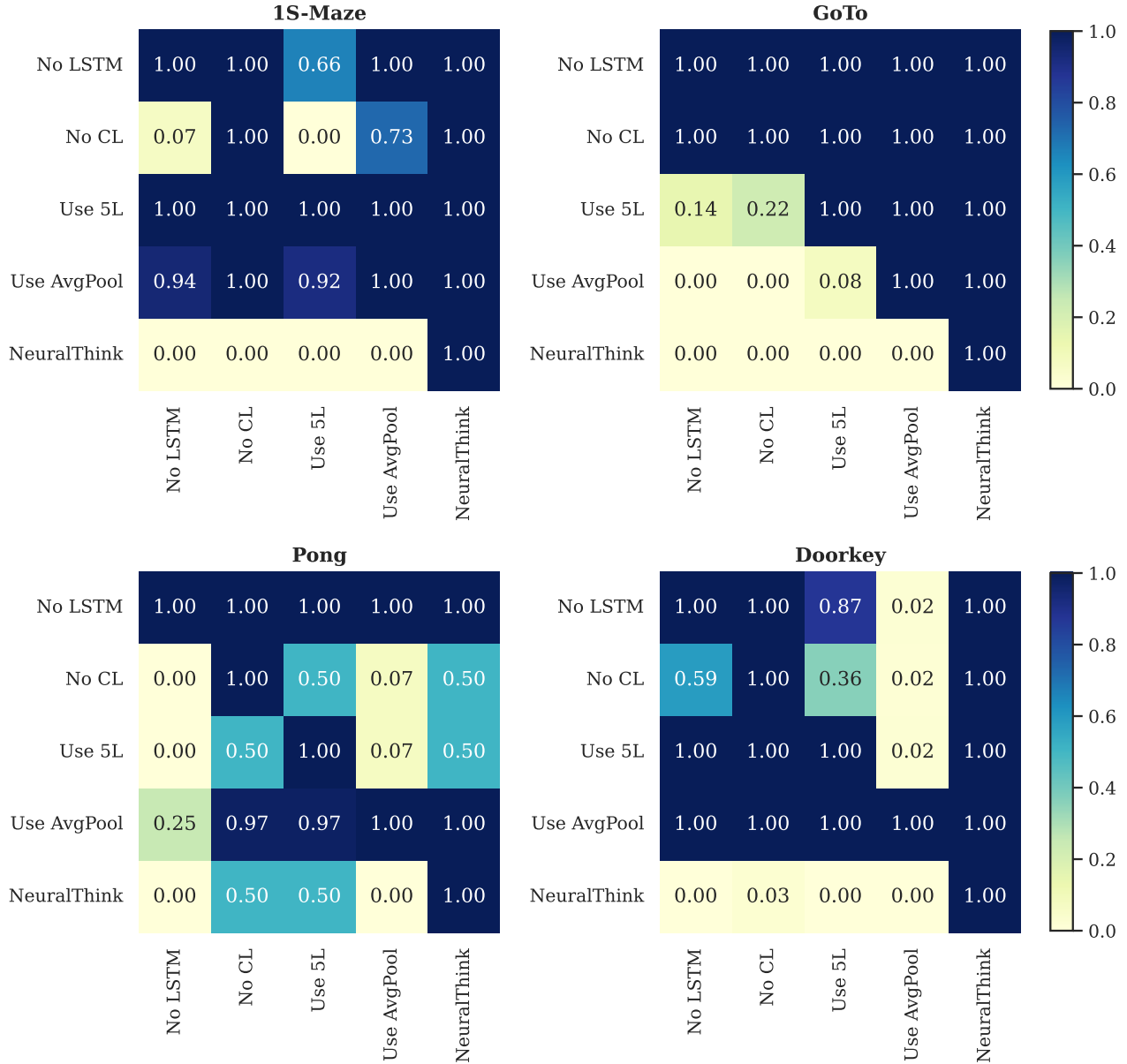


Figure 12: Almost Stochastic Order scores of the ablation study on the asymmetrical tasks. ASO scores are expressed in ϵ_{\min} , with a significance level $\alpha = 0.05$ that is adjusted accordingly by using the Bonferroni correction (Bonferroni, 1936). Read from row to column: E.g., NeuralThink (row) is stochastically dominant over No LSTM (column) in the 1S-Maze task with ϵ_{\min} of 0.00.

G.4. Extrapolation on Sequential Decision-Making Tasks

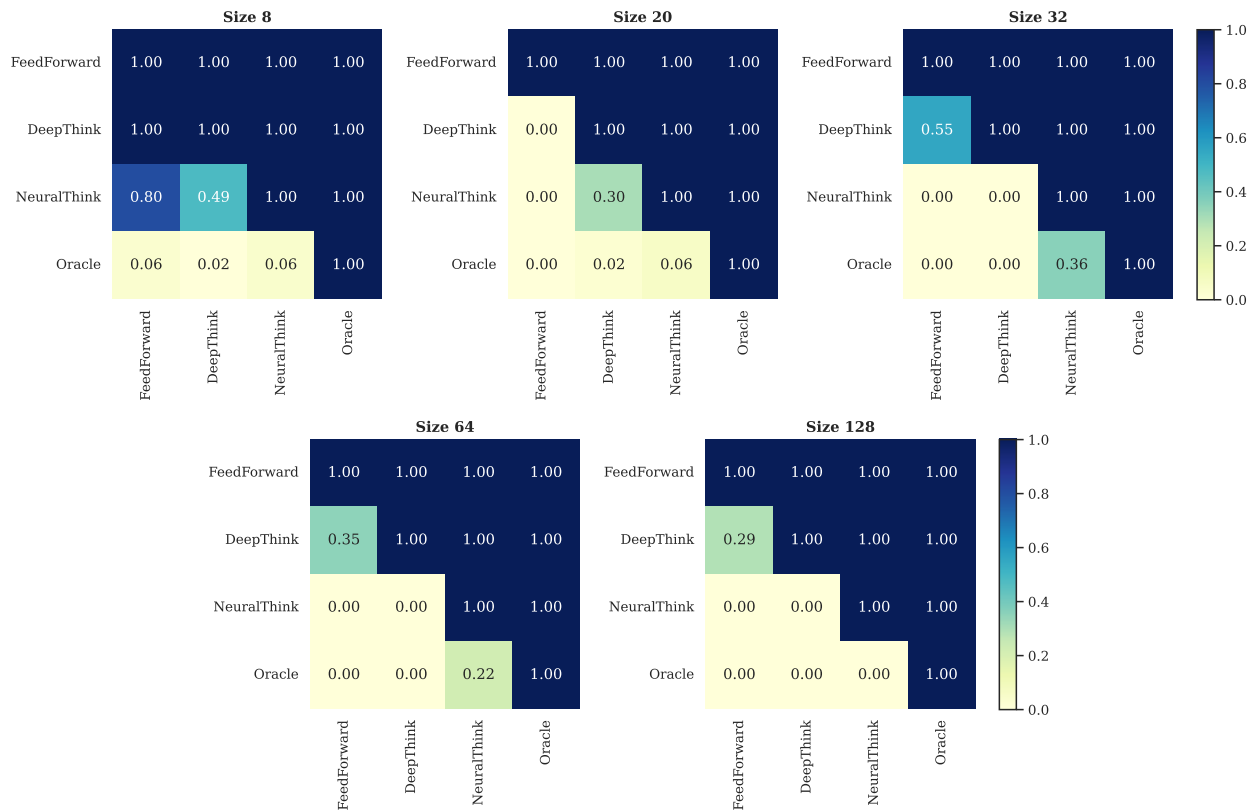


Figure 13: Almost Stochastic Order scores of the Doorkey sequential decision-making task results. ASO scores are expressed in ϵ_{\min} , with a significance level $\alpha = 0.05$ that is adjusted accordingly by using the Bonferroni correction (Bonferroni, 1936). Read from row to column: E.g., NeuralThink (row) is stochastically dominant over DeepThink (column) starting at size 32 with an ϵ_{\min} of 0.00.

G.5. Fine-tuning of the Progressive Loss Parameter

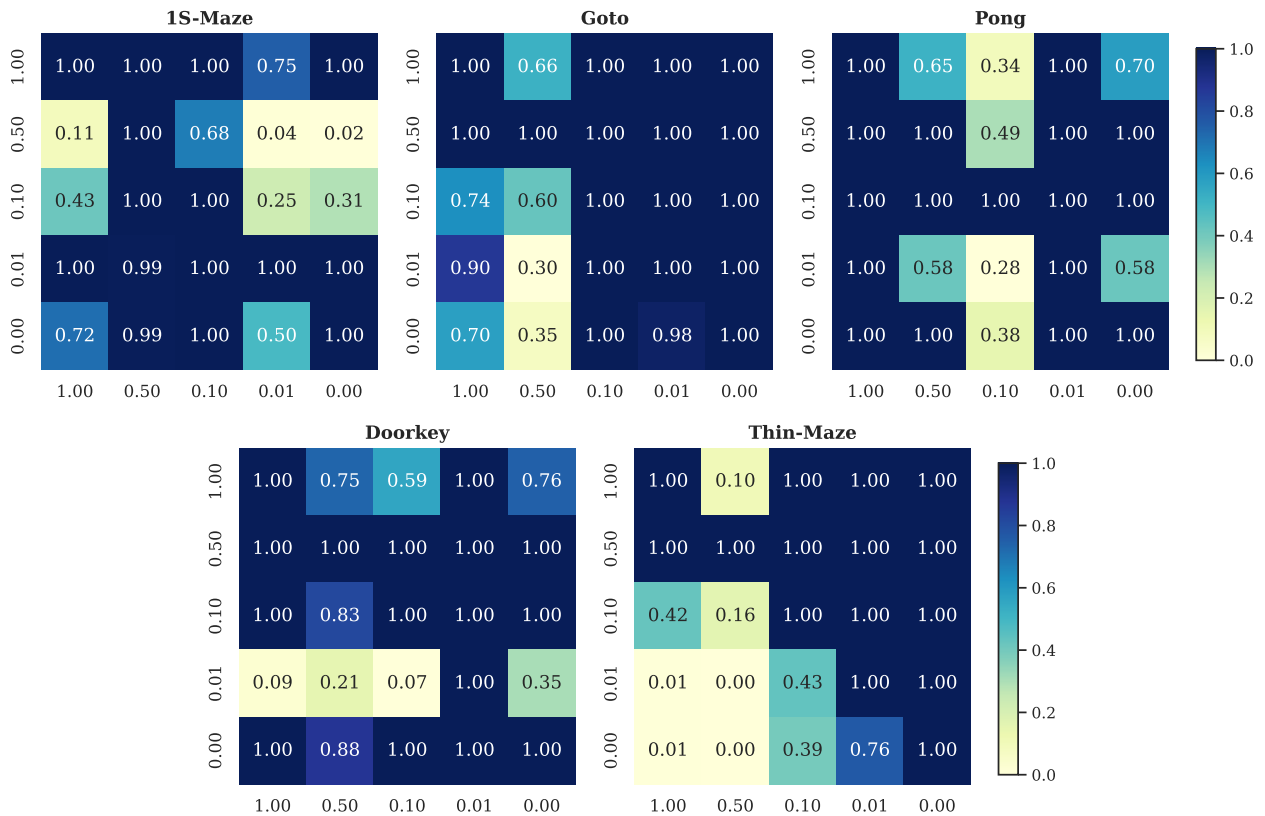


Figure 14: Almost Stochastic Order scores of the fine tuning progressive loss results. ASO scores are expressed in ϵ_{\min} , with a significance level $\alpha = 0.05$ that is adjusted accordingly by using the Bonferroni correction (Bonferroni, 1936). Read from row to column: E.g., a progressive loss alpha value of 0.5 (row) is almost stochastically dominant over the value of 1. (column) in the 1S-Maze task with ϵ_{\min} of 0.11.

H. Looking Inside the Latent Space

In this section, we show a visualization of the latent space of the NeuralThink model while solving the asymmetrical tasks. More specifically, we visualize the difference between the current latent state and the last latent state, for each recurrent iteration. The following figures show two plots per iteration: the one on top shows the difference between the recurrent states in a certain color superimposed over the input image, while the one below shows the predicted action probabilities outputted by the model.

With these visualizations we notice how the information propagates through the input problems, giving a hint of the algorithm that the model is performing. An interesting observation across these visualizations is how the final prediction of the model only converges to the correct action after the recurrent iterations have converged to a fixed state around the player position.

H.1. 1S-Maze

By looking at how the information propagates through the maze paths in Figure 15 and 16, the model appears to learn a parallel algorithm that starts with the dead ends until finding the optimal path between the player (green) and the goal (red). At iteration #90 in Figure 15, the visible difference between the current and last recurrent states actually represents the optimal path between the player and the goal. The algorithm converges to the optimal task after the difference of the state converges near the player. Figure 16 shows that finding the optimal path is not necessary to predict the next action.

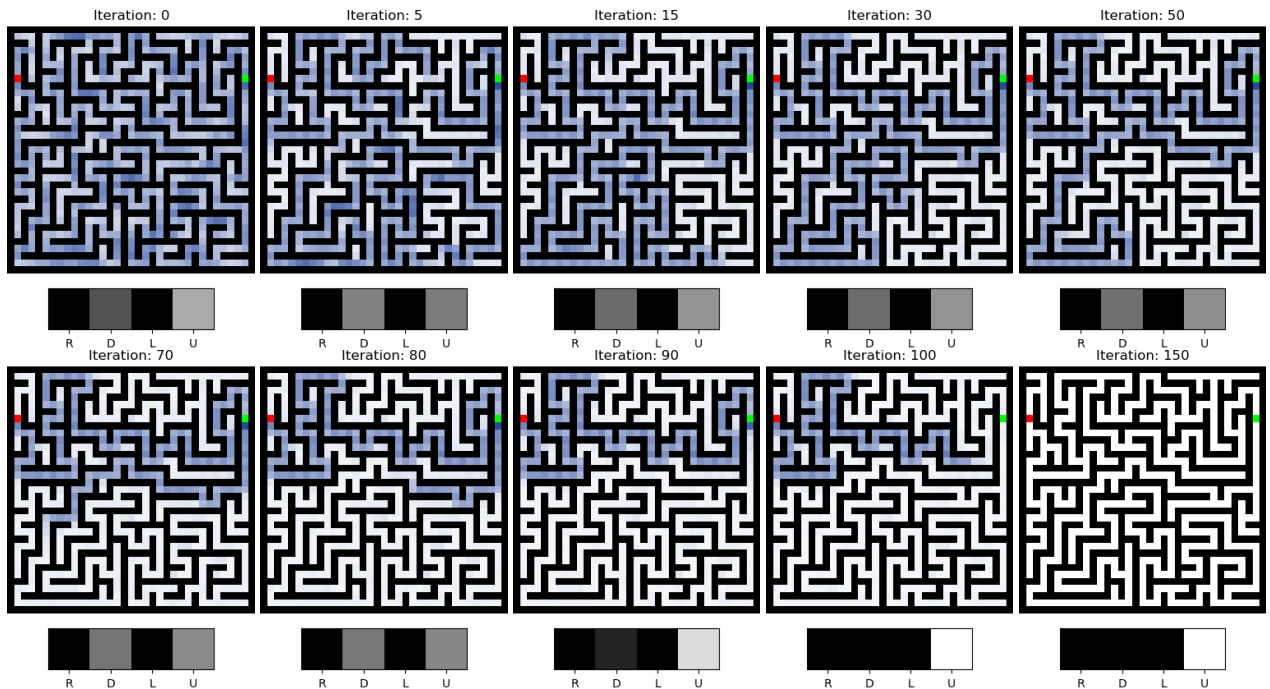


Figure 15: Visualization in dark blue of the difference between the current iteration and last iteration (iteration number 200, not represented) of the recurrent state of NeuralThink, on the 1S-Maze task of size 35x35. The white pixels represent the pixel positions of the recurrent state that converged to a fixed final state. Below the maze are the predicted action probabilities outputted by the model at respective iteration, namely Right (R), Down (D), Left (L), and Up (U).

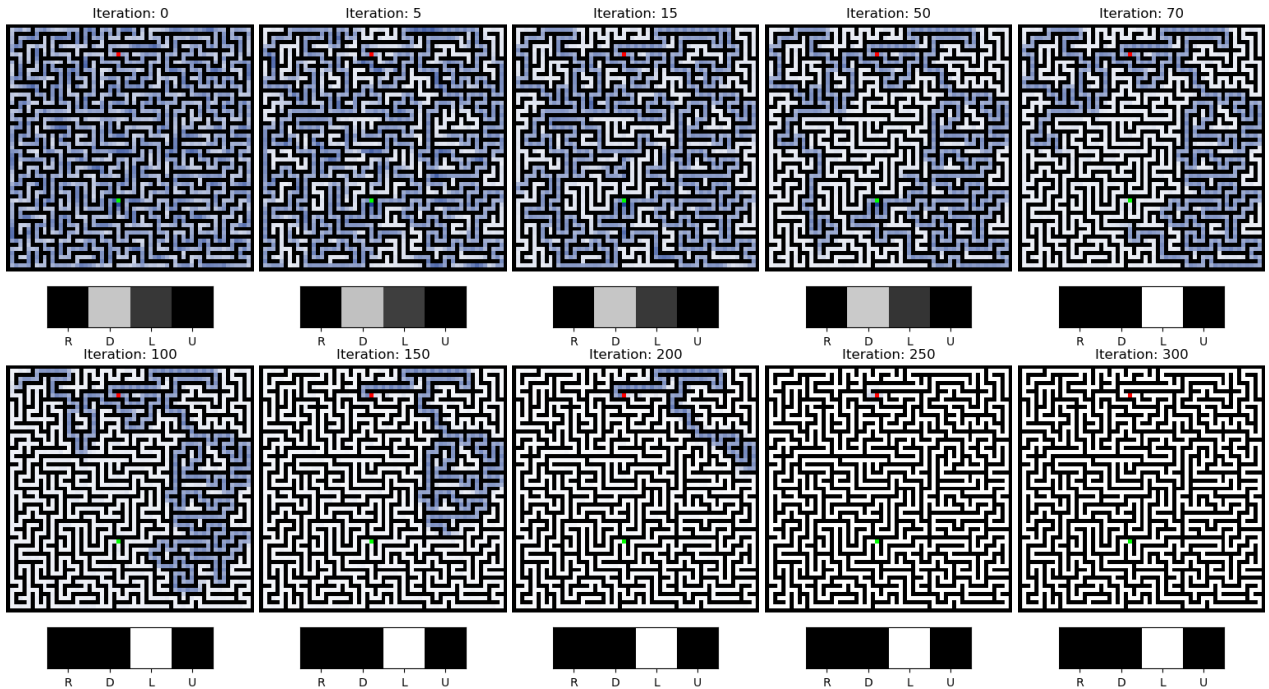


Figure 16: Visualization in dark blue of the difference between the current iteration and last iteration (iteration number 1000, not represented) of the recurrent state of NeuralThink, on the 1S-Maze task of size 61×61 . The white pixels represent the pixel positions of the recurrent state that converged to a fixed final state. Below the maze are the predicted action probabilities outputted by the model at respective iteration, namely Right (R), Down (D), Left (L), and Up (U).

H.2. Goto

In this section, we show 3 examples of possible player and goal positions that influence the final predicted action. Namely, if the player (green) is above the goal (red), below the goal, or at the same level in height.

In Figure 17, we can notice that the model chooses by default the up action, while across the iterations a signal is sent from the goal position to the positions above, propagating in a circular/oval shape. Thus the model appears to learn an algorithm that attempts to signal the player if it should go down. This logic is proved in Figure 18, where the recurrent state does not change near the player, as such the predicted action remains the same.

In Figure 19 we see a case in which the player is on the left of the goal. In this setting, the horizontal line with a slightly different contrast ranging from the goal position appears to communicate across that line the player should go left or right to reach the goal.

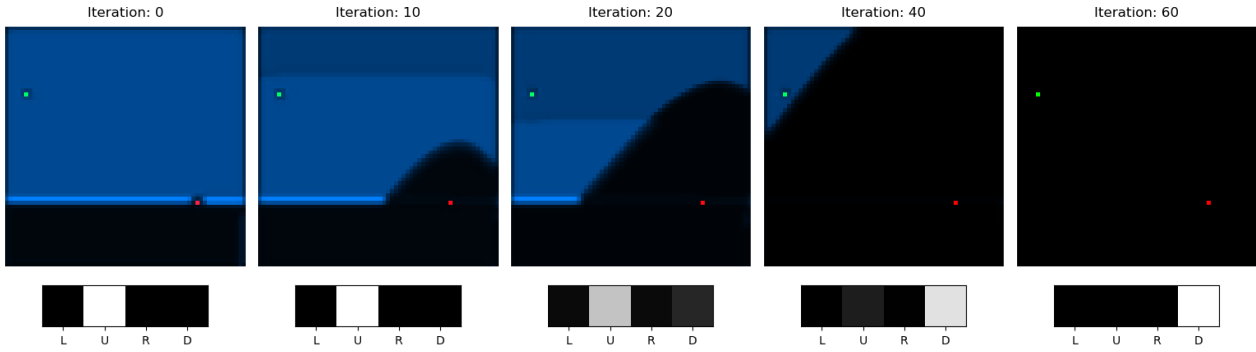


Figure 17: Visualization in dark blue of the difference between the current iteration and last iteration (iteration number 200, not represented) of the recurrent state of NeuralThink, on the GoTo task of size 64×64 . The black pixels represent the pixel positions of the recurrent state that converged to a fixed final state. Below the figure are the predicted action probabilities outputted by the model at respective iteration, namely Left (L), Up (U), Right (R), and Down (D).

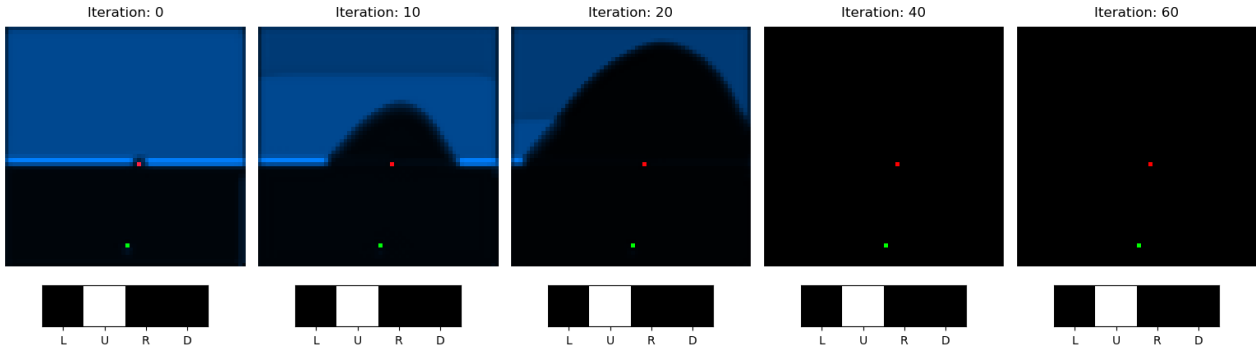


Figure 18: Visualization in dark blue of the difference between the current iteration and last iteration (iteration number 200, not represented) of the recurrent state of NeuralThink, on the GoTo task of size 64×64 . The black pixels represent the pixel positions of the recurrent state that converged to a fixed final state. Below the figure are the predicted action probabilities outputted by the model at respective iteration, namely Left (L), Up (U), Right (R), and Down (D).

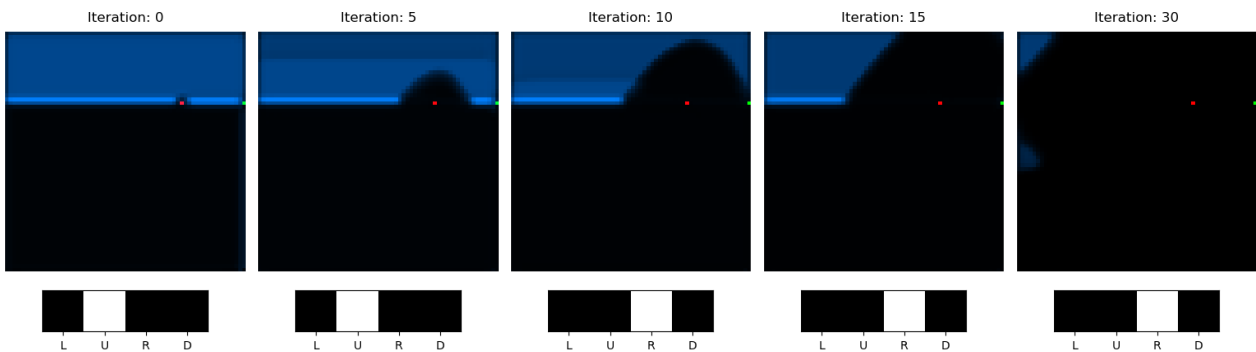


Figure 19: Visualization in dark blue of the difference between the current iteration and last iteration (iteration number 200, not represented) of the recurrent state of NeuralThink, on the GoTo task of size 64×64 . The black pixels represent the pixel positions of the recurrent state that converged to a fixed final state. Below the figure are the predicted action probabilities outputted by the model at respective iteration, namely Left (L), Up (U), Right (R), and Down (D).

H.3. Pong

In this section, we present two examples of NeuralThink solving the simplified game of pong: one when the ball is on the left of the paddle, and the other when on the right. We can notice that the model appears to learn a similar algorithm to the model in the GoTo task. In both Figures the model starts by predicting that the paddle should move right. In Figure 20, the model prediction changes once the information propagation reaches the paddle, changing it to the left action. In Figure 21, we see that this propagation of information does not reach the paddle, and as such the action remains unchanged.

We can also see a line with a slightly different contrast leaving the center of the ball, thus signaling that the model should instead predict the stay action. This could indicate that different contrasts might represent different algorithms. We leave as future work investigating in more depth the possible algorithms that these models can learn.

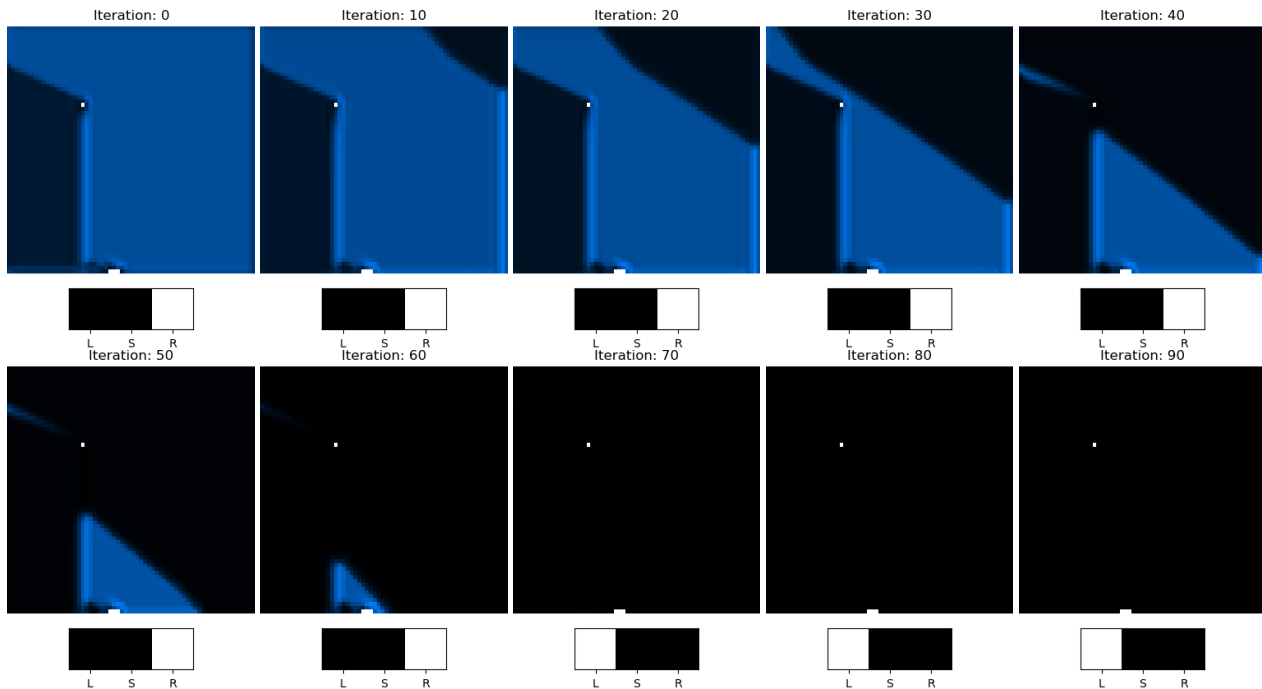


Figure 20: Visualization in dark blue of the difference between the current iteration and last iteration (iteration number 200, not represented) of the recurrent state of NeuralThink, on the Pong task of size 64×64 . The black pixels represent the pixel positions of the recurrent state that converged to a fixed final state. Below the figure are the predicted action probabilities outputted by the model at respective iteration, namely Left (L), Stay (S), and Right (R).

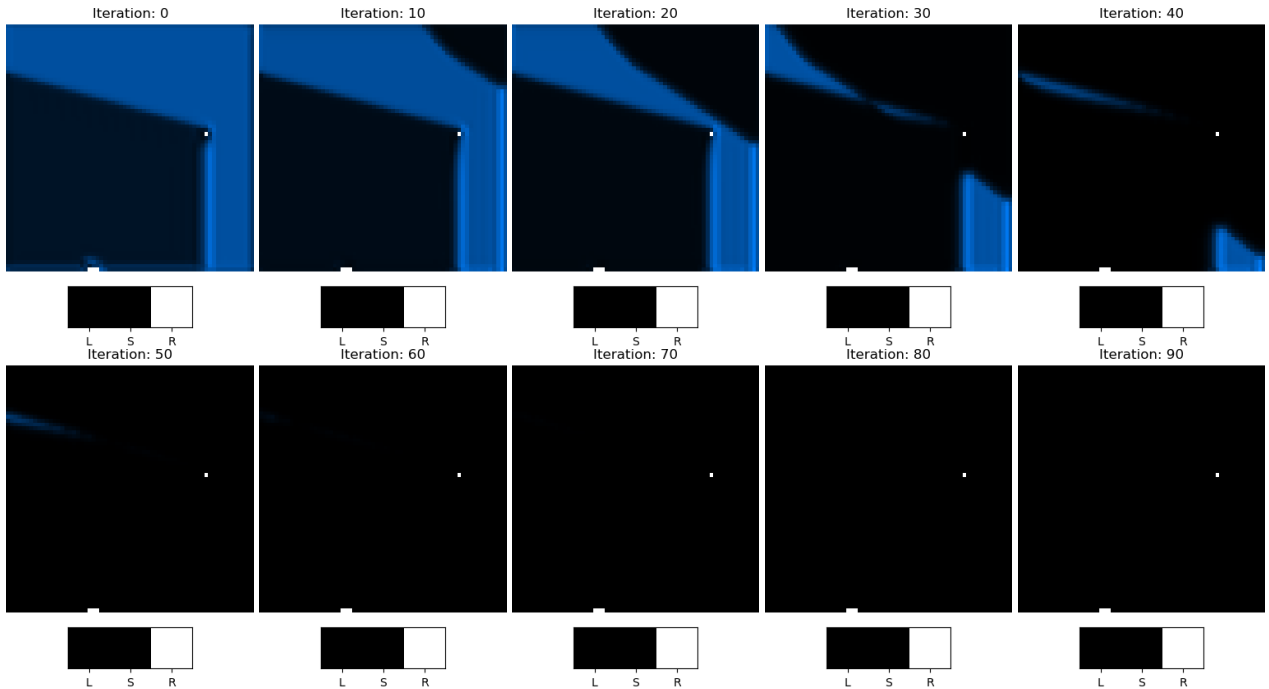


Figure 21: Visualization in dark blue of the difference between the current iteration and last iteration (iteration number 200, not represented) of the recurrent state of NeuralThink, on the Pong task of size 64×64 . The black pixels represent the pixel positions of the recurrent state that converged to a fixed final state. Below the figure are the predicted action probabilities outputted by the model at respective iteration, namely Left (L), Stay (S), and Right (R).

H.4. Doorkey

In this section, we provide two examples of doorway input problems: in Figure 22 we show when the player is almost reaching the goal, and in Figure 23 when it already captured the key and is reaching for the door.

We notice that these visualizations are harder to interpret than the other ones. This might also occur since to solve this task, the agent needs to follow a complex sequence of tasks, thus requiring multiple algorithms to find where the positions of the objects are and which action to do next. Not only that, but how for example not having the key present in the grid might prevent the execution of certain information propagating algorithms. We can notice this in Figure 23, where there is a line that shoots vertically from the door position that is not present in Figure 22. This shows that for more complex tasks, better visualization and interpretation techniques of the recurrent states are required.

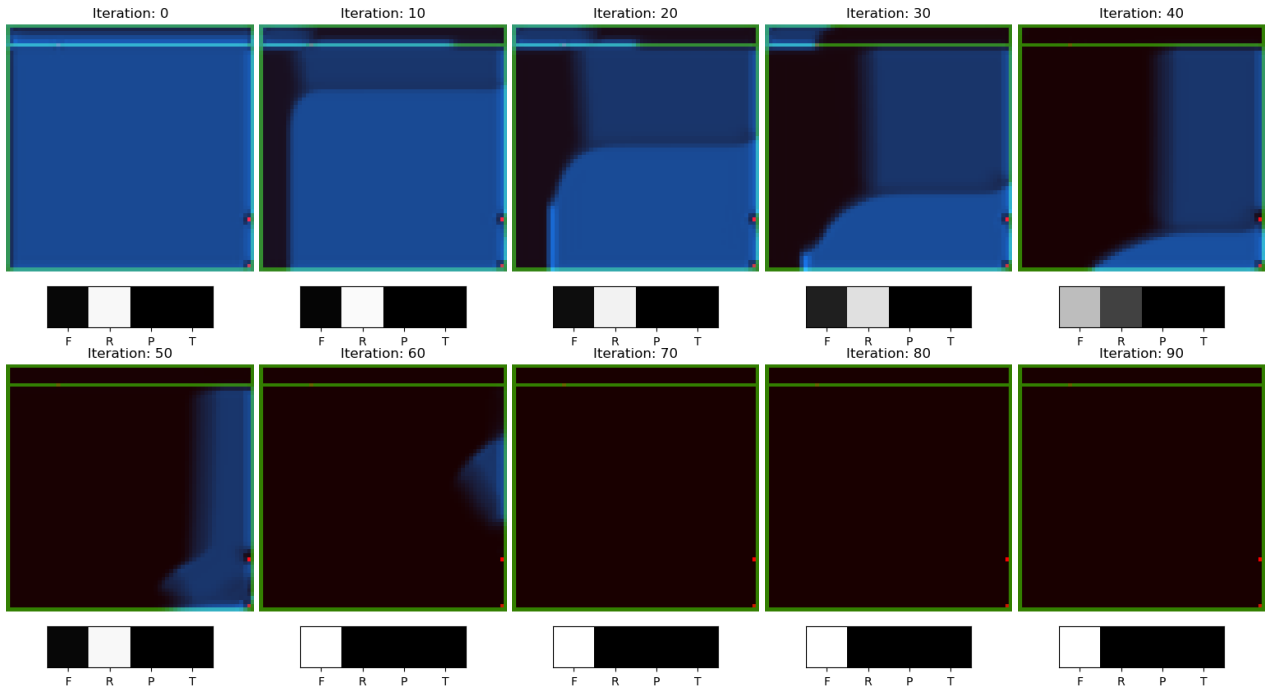


Figure 22: Visualization in dark blue of the difference between the current iteration and last iteration (iteration number 200, not represented) of the recurrent state of NeuralThink, on the Doorkey task of size 64×64 . The black pixels represent the pixel positions of the recurrent state that converged to a fixed final state. Below the grid are the predicted action probabilities outputted by the model at respective iteration, namely Forward (L), Rotate Right (R), Pickup (P), and Toggle (T).

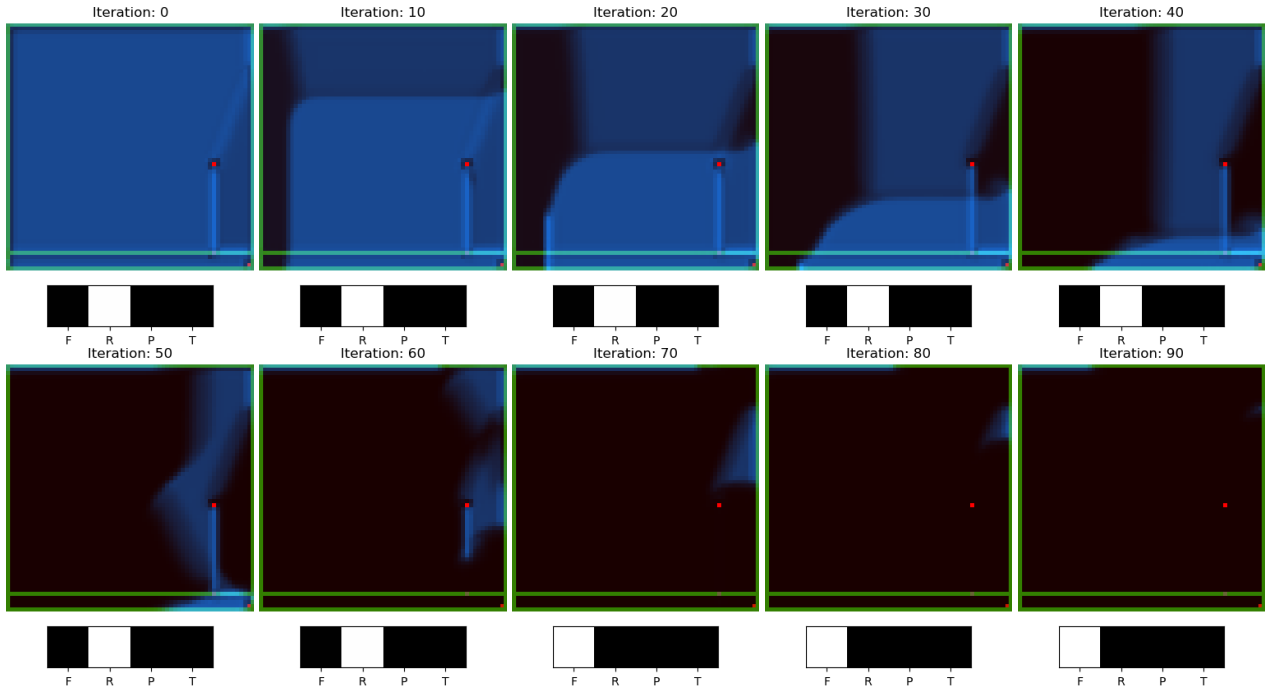


Figure 23: Visualization in dark blue of the difference between the current iteration and last iteration (iteration number 200, not represented) of the recurrent state of NeuralThink, on the Doorkey task of size 64×64 . The black pixels represent the pixel positions of the recurrent state that converged to a fixed final state. Below the grid are the predicted action probabilities outputted by the model at respective iteration, namely Forward (L), Rotate Right (R), Pickup (P), and Toggle (T).

I. Additional Example Trajectories

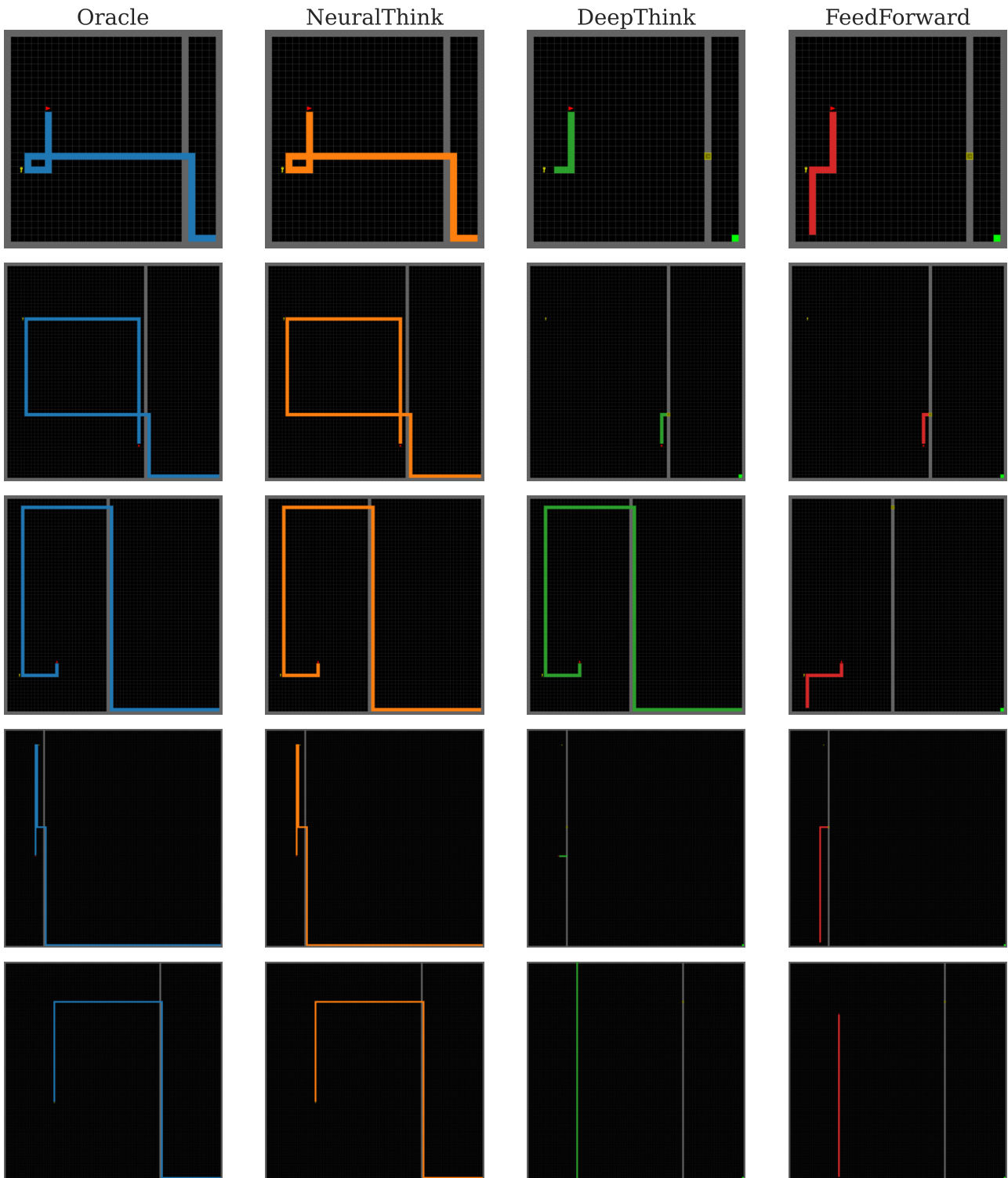


Figure 24: Visualization of the trajectories of NeuralThink, DeepThink, and FeedForward models against the Oracle trajectory. The first row is a task of size 32×32 , second and third of 64×64 , and fourth and fifth of 128×128 . In this small example set, only NeuralThink continuously matches the Oracle trajectories.

J. Examples of tasks of size 512

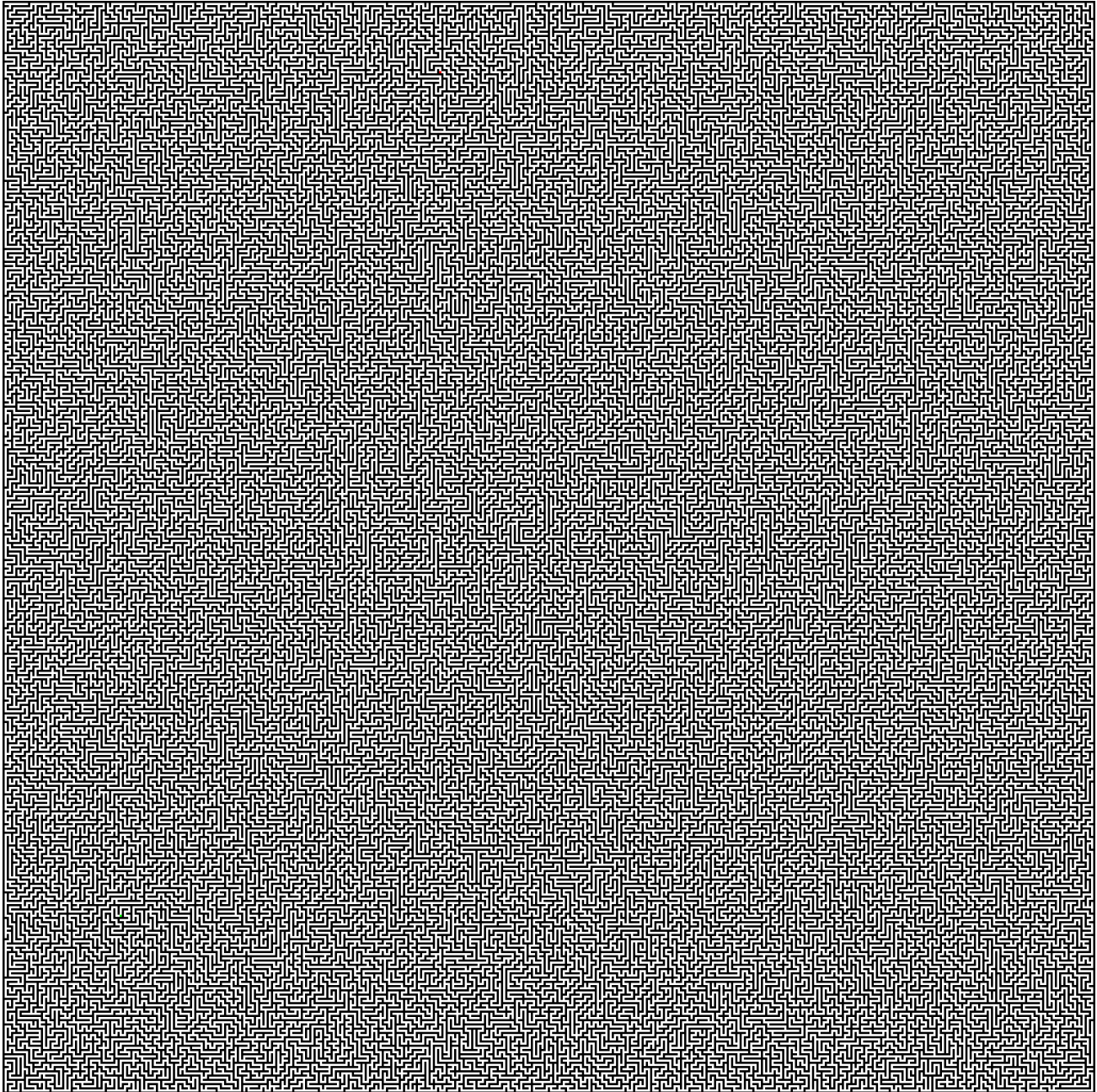


Figure 25: Example of a 512 size maze task

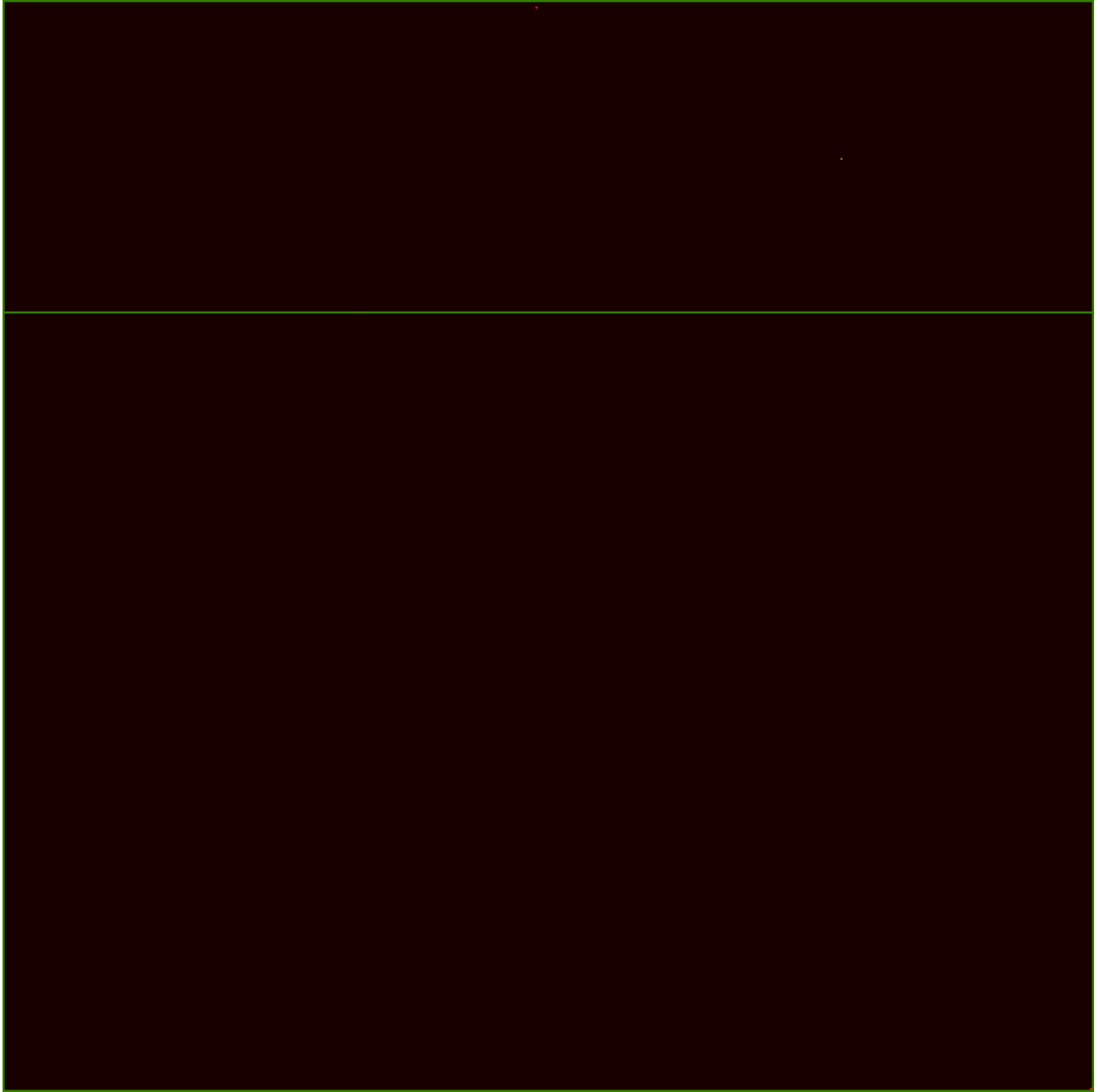


Figure 26: Example of a 512 size doorkey task